Resistance of submerged groynes

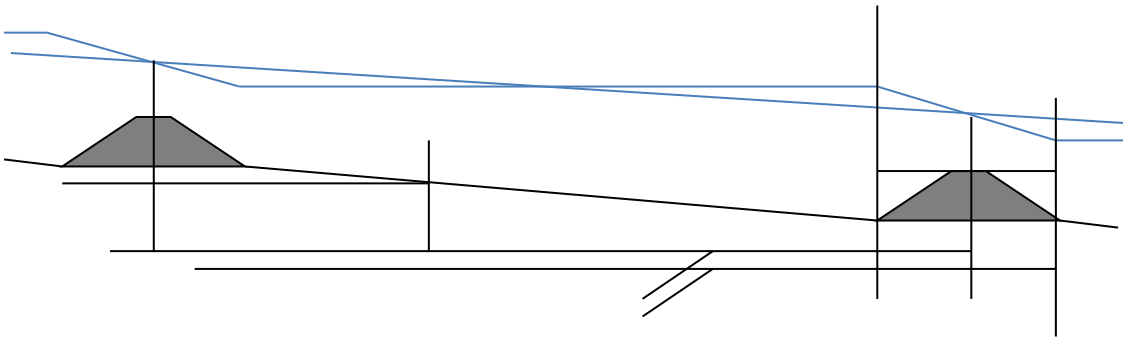

Maurits Kruijt
July 2013

TU Delft Delft University of Technology

MSc Thesis
Maurits Kruijt, July 2013

Resistance of submerged groynes

Thesis committee:
Prof. dr. ir. W.S.J. Uijttewaal
Dr. ir. M. Zijlema
Dr. ir. B.C. van Prooijen

Summary

Groynes are commonly used in the major rivers in the Netherlands. They confine the flow of the river to a main channel but also act as resistance element once submerged and in that way influence the stage discharge relationship of the river. Several formulas exist describing groynes as a drag resistance. Another possible way of determining their resistance is by using a weir formula and fitting the up and downstream water levels to the water level slope of the river.

In this thesis a schematized model of the river Waal is set up and progressively expanded. At first seven different drag and weir formulas are compared. There is no consensus for resistance is between them. They are therefor compared to a 2DV computer model of flow over a highly submerged weir in the SWASH software package. Drag resistance, expressed as a function of water depth to groyne height ratio has the same scaling as two weir formulas though they do not match in absolute terms.

A 2DH computer model is then used to determine the magnitude of the lateral turbulent momentum exchange between the main channel, groyne fields and flood plain.
Finally a 3D computer model is used to determine groyne resistance and the distribution of discharge and momentum around the groyne. Treating groynes as weirs is found to be an acceptable assumption.

The schematized model is used to simulate a high discharge of 13.550 $m^3 s^{-1}$. Groynes, when seen as a weir, would be responsible for a 36 cm water level increase. Lateral turbulent momentum exchange increases this by another 34 cm, while using the groyne resistance found in the 3D model added only another 7 cm.

Contents

1	Introduction		4
	1.1	General	4
	1.2	Problem description	4
	1.3	Goal	5
	1.4	Research approach	6
2	Flow in rivers		7
	2.1	Basic equations	7
	2.2	1D compound channel model	10
	2.3	Groynes as drag resistance	11
	2.4	Groynes as weirs	13
	2.5	Horizontal momentum exchange	17
3	Formulas for groyne resistance		21
	3.1	Groynefield geometry	21
	3.2	Overview of formulas	22
	3.3	Resistance	25
	3.4	Sensitivity of formulas	26
	3.5	Conclusions	34
4	1D river model		36
	4.1	Computer model of flow over a single groyne	36
	4.2	Schematized model	39
	4.3	Conclusions	41
5	2D river model		43
	5.1	2DH computer model	43
	5.2	Schematized model	50
	5.4	Conclusions	51
6	3D river model		52
	6.1	3D computer model	52
	6.2	Schematized model	58
	6.3	Conclusions	60
7	Conclusions		61
8	Recommendations		63
9	References		64

1 Introduction

1.1 General

Groynes are commonly used in the major rivers in the Netherlands. The function of these structures is to direct the main flow away from the banks. Thereby creating a deep main channel suitable for navigation and preventing erosion that would result in the natural meandering of the river. During low discharges in summer they are emerged and can easily be seen. During the high discharges in winter they are submerged and contribute to flow resistance.

The "Room for the Rivers" project of Rijkswaterstaat aims to reduce the flood risk of rivers. One of the measures is to reduce the height of groynes in certain river sections. The reasoning being that since groynes behave as resistance elements reducing their height, and thus resistance, will lead to a lower water level for a certain discharge. In order to predict the effect of such a measure this resistance should of course be known.

Formulas for groyne resistance have been found through flume tests such as those of Yossef (2005) and Azinfar (2010), or numerically by Van Broekhoven (2007). All three included a drag coefficient that represents a myriad of effects that together make up the resistance of groynes in a river system. To find and effectively model the resistance of groynes it should be understood which processes and parameters determine this coefficient.

Another way of looking at submerged groynes is considering them to behave as the more well studied weirs, such as done by Mosselman & Struiksma (1992). The obvious difference is that flow can go around as well as over groynes and groynes can come in series. This makes it questionable if groynes can be represented as weirs and if the knowledge about the behavior of weirs is sufficient for simply studying groynes.

1.2 Problem description

Groynes are common in Dutch rivers and influence the stage discharge relationship. In order to reduce flood risk at high discharges ministry of public works is reducing groyne height. To predict the effect of such a measure a good description of groyne resistance is needed, yet information about it is scarce.

Three studies (Yossef 2005, Van Broekhoven 2007 and Azinfar 2010) compared groyne resistance to a drag resistance dependent on varying flow and geometrical parameters. Another way of looking at groyne resistance is to compare them to the more well studied weirs as was done by Mosselman & Struiksma (1992). Bloemberg (2001) and Fritz & Hager (1998) studied flow over submerged broad crested weirs.

Flow over groynes differs from flow over weirs however. Firstly groynes do not extend over the full width of the flow and secondly in Dutch rivers multiple groynes in succession, or groyne fields, are used. This can be seen in figure 1.1. This arrangement causes a large amount of turbulence on the interface between groyne fields and main flow with a large gyre (or large coherent structure) between subsequent groynes. If a large

amount of streamwise momentum simply goes around the groyne instead of over it, this would make using weir formulas in this case questionable.

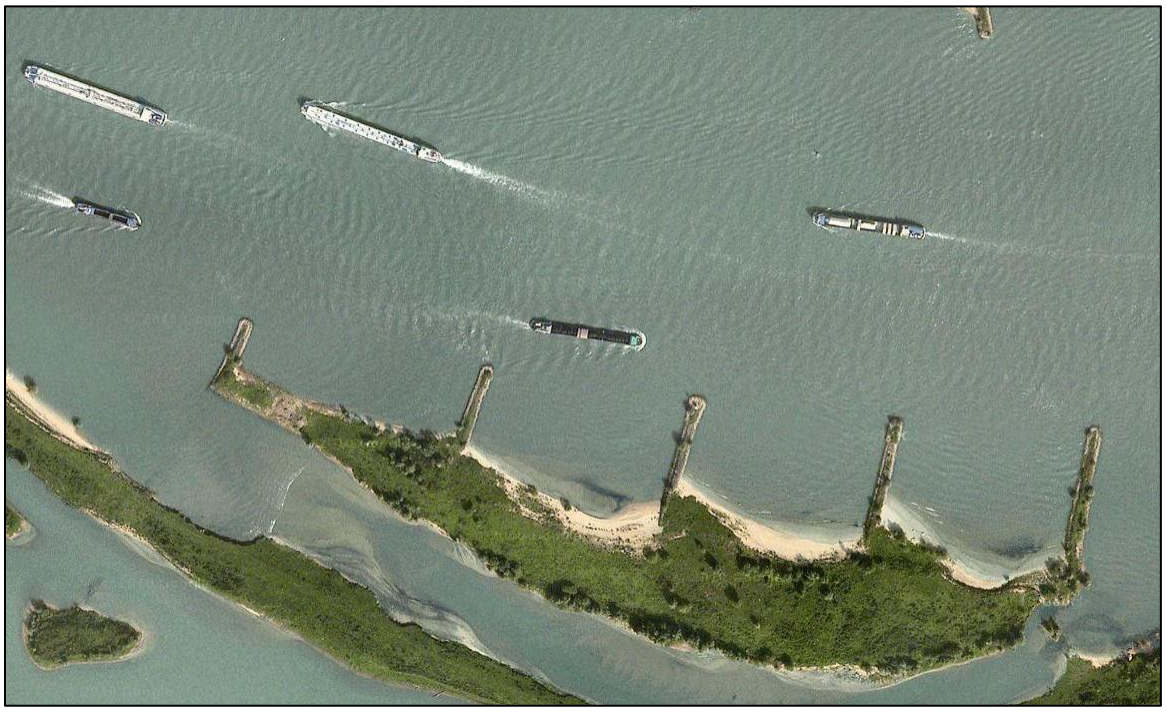

Figure 1.1: A series of groynes in the river Waal near Haaften. Souce: Google maps.

These issues come together in modeling. To determine the stage-discharge relationship of a river with groynes the computer model must either have a fine grid and include groynes in the bottom topography, or, if a course grid is used, groyne resistance must be approximated with a formula. WAQUA, used by Rijkswaterstaat does this by using a weir formulation to calculate energy loss, which is then turned into a higher bottom resistance.

1.3 Goal

The aim of this thesis is to determine what makes up the resistance of submerged groynes, and on which parameters it depends. The second aim is to determine if flow over groynes can be compared to flow over weirs even if horizontal momentum exchange plays a role.

The following research questions have been formulated:
1. What is the resistance of submerged groynes and on which parameters does this depend?
2. What is the magnitude of horizontal momentum exchange by large coherent structures?
3. Can groynes be seen as weirs? If so, which formulation is most applicable?

1.4 Research approach

A schematized model of the river Waal is set up and progressively expanded. The basic theory needed to understand flow in rivers and the setup of this model is explained in chapter 2.

A literature review will be conducted to provide an estimate for the resistance of submerged groynes. This knowledge is used in chapter 3 to compare known resistance formulas of groynes and weirs to see which of these are useful. Based on these formulas an estimate can be made of how important different flow and geometry parameters are.

After that a schematized model for flow in the river Waal is compared to computer simulations. The first step is comparing it to a 2DV simulation of flow over heavily submerged weirs using the SWASH software. This is found in chapter 4.

A 2DH computer model is used to determine turbulent momentum exchange between different river sections. This is added to the schematized model in chapter 5.

The discharge in groyne fields will also be studied to find how this divides itself into flow going over and flow going around the groynes. This is done using a 3D computer model and will be used to determine if flow in groyne fields can be described using discharge formulas for weirs. This is covered in chapter 6.

2 Flow in rivers

In this thesis a schematized model of a river will be used and compared to a computer model. The setup of this schematized model will be explained in this chapter. It is based on a 1D model of a compound channel. It is expanded to included groyne resistance, either as drag resistance or as a weir, as well as horizontal momentum exchange due to turbulence.

2.1 Basic equations

Starting point for the describing flow in rivers are the continuity (2.1) and horizontal momentum (2.2 and 2.3) equations for incompressible flows. The explanation below follows that of Jansen (1979).

$$\frac{\partial u}{\partial x}+\frac{\partial v}{\partial y}+\frac{\partial w}{\partial z}=0 \tag{2.1}$$

$$\frac{\partial u}{\partial t}+\frac{\partial u^2}{\partial x}+\frac{\partial uv}{\partial y}+\frac{\partial uw}{\partial z}+g\frac{\partial z_w}{\partial x}=0 \tag{2.2}$$

$$\frac{\partial v}{\partial t}+\frac{\partial uv}{\partial x}+\frac{\partial v^2}{\partial y}+\frac{\partial vw}{\partial z}+g\frac{\partial z_w}{\partial y}=0 \tag{2.3}$$

u, v, w	=	Velocity in x, y and z direction	[m s^{-1}]
g	=	Gravitational constant equal to 9.81	[m s^{-2}]
z_w	=	Water level	[m]

It is very time consuming to model the small turbulent scales present in fluid flows. A solution to this is Reynolds decomposition. The velocity components u, v, and w are now separated in a time averaged ($\tilde{u}$) and a turbulent (u') component (2.4).

$$u=\tilde{u}+u', \text{ etc} \tag{2.4}$$

After time averaging this leads to the following equations of motion:

$$\frac{\partial \tilde{u}}{\partial x}+\frac{\partial \tilde{v}}{\partial y}+\frac{\partial \tilde{w}}{\partial z}=0 \tag{2.5}$$

$$\frac{\partial \tilde{u}}{\partial t}+\frac{\partial \tilde{u}^2}{\partial x}+\frac{\partial \tilde{u}\tilde{v}}{\partial y}+\frac{\partial \tilde{u}\tilde{w}}{\partial z}+g\frac{\partial z_w}{\partial x}+\frac{\partial \widetilde{u'^2}}{\partial x}+\frac{\partial \widetilde{u'v'}}{\partial y}+\frac{\partial \widetilde{u'v'}}{\partial z}=0 \tag{2.6}$$

$$\frac{\partial \tilde{v}}{\partial t}+\frac{\partial \tilde{u}\tilde{v}}{\partial x}+\frac{\partial \widetilde{v^2}}{\partial y}+\frac{\partial \tilde{v}\tilde{w}}{\partial z}+g\frac{\partial z_w}{\partial x}+\frac{\partial \widetilde{u'v'}}{\partial x}+\frac{\partial \widetilde{v'^2}}{\partial y}+\frac{\partial \widetilde{v'w'}}{\partial z}=0 \tag{2.7}$$

Three new terms have appeared in the momentum equations as a result of performing this this operation on the advection terms. These represent the exchange of momentum between adjacent areas of the flow due to turbulent fluctuations. When multiplied with the density ρ they take the shape of a shear stress and are then called the Reynolds stresses (2.8).

$$\widetilde{u'v'} = -\frac{1}{\rho}\tau_{xy}, \text{ etc} \qquad (2.8)$$

ρ	=	Density	[kg m^{-3}]
τ	=	Shear stress	[N m^{-2}]

While this set of equations can be used to describe flow in a river, a computer would be needed to solve these. A far simpler relationship exists that can be solved analytically. If the flow can be assumed steady ($\frac{\partial(\dots)}{\partial t} = 0$), uniform ($\frac{\partial(\dots)}{\partial x} = 0$) and two-dimensional ($\frac{\partial(\dots)}{\partial y} = 0$). Formula 2.6 is then reduced to:

$$g\frac{\partial z_w}{\partial x} - \frac{1}{\rho}\frac{\partial \tau_{xz}}{\partial z} = 0 \qquad (2.9)$$

At the bottom the shear stress is given by the bottom shear stress, while at the water surface there is assumed to be none (no wind). This leads to the following distribution over the vertical:

$$\tau_{xz} = \tau_b\left(1 - \frac{z}{d}\right) \qquad (2.10)$$

d	=	Water depth	[m]

This allows formula 2.9 to be integrated over the vertical leading to:

$$\tau_b = -\rho g d\frac{\partial z_w}{\partial x} \qquad (2.11)$$

In other words the pull of gravity on the body of water is balanced out by the bottom shear stress. In order to solve this equation an expression must be found for the Reynolds stresses in terms of the main flow field. This known as the turbulence closure problem. This will looked at in more detail in section 2.5 for the horizontal stresses, for now only the vertical is considered. One solution is the eddy viscosity concept, whereby Reynolds stresses are compared a viscous stress:

$$\tau_{xz} = \rho\upsilon_t\frac{\partial u}{\partial z} \qquad (2.12)$$

υ_t	=	Turbulent viscosity	[m^2 s^{-1}]

This in turn introduces the turbulent viscosity, which must then be described further. One relatively simple approach is the model of Prandtl where it is a function of mixing length and velocity gradient.

$$\upsilon_t = l_m^2\frac{\partial u}{\partial z} \qquad (2.14)$$

l_m = Mixing length [m]

For regions close to the wall, or in this case the bottom, mixing length is related to the distance to the wall:

$$l_m = \kappa z \tag{2.15}$$

κ = Von Kárman's constant, equal to 0.41 [-]

This relationship can be used to derive a logarithmic velocity profile over the vertical. For a full derivation see Jansen (1979). What is important to know is that for such a flow in a river an empirical relationship exists between the bottom shear stress and the depth averaged velocity ($\bar{u}$):

$$\frac{\tau_b}{\rho} = \frac{g}{C^2}\bar{u}^2 \tag{2.16}$$

C = Chézy coefficient [$m^{0.5}$ s^{-1}]

Combined with formula 2.11 this leads to the Chézy's law. Since uniform flow was assumed, the water level slope ($\frac{\partial z_w}{\partial z}$) is equal to the bottom level slope (i):

$$\bar{u} = C\sqrt{di} \tag{2.17}$$

i = Bottom level slope [m]

The value of the Chézy coefficient can be found with the following empirical relationship:

$$C = 10\log_{10}\left(\frac{12d}{k_s}\right) \tag{2.18}$$

k_s = Nikuradse bottom roughness [m]

Chézy's law forms the basis of the model that will be used in this thesis. In the following sections if will be expanded to accommodate different river sections, groynes and horizontal momentum exchange. In the remainder of this thesis all properties, unless noted otherwise are assumed to be time averaged. Depth averaging will still be denoted by an overbar ($\bar{...}$).

2.2 1D compound channel model

The river Waal is a branch of the Rhine river in the Netherlands. During low discharges in summer flow is confined to the deep main channel with the aid of groynes and small summer dikes (figure 2.1). During high discharges in the winter these are overtopped and water flows through the flood plain as well. In that case streamwise velocity varies quite a bit over the cross-section due to changes in water depth and bed roughness. Van der Wal (2004) for example gives values of 2.5 m/s for the main channel to 0.2 m/s for the floodplains.

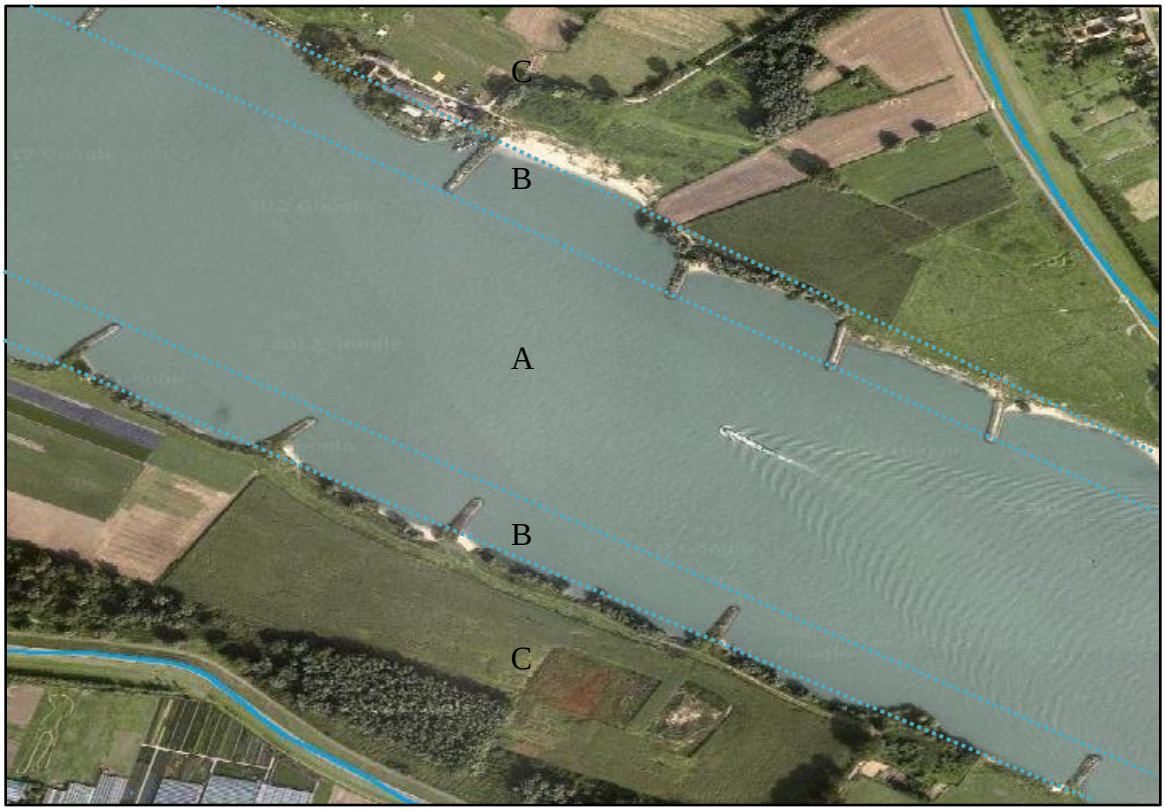

Figure 2.1: River Waal during low discharge with (A) main channel, (B) groyne fields and (C) floodplains marked, source: Google Maps.

To deal with this the river is divided into three parts: the main channel, groyne fields and the flood plain. In each of these parts Chézy's law (formula 2.17) is used. The sum of all three parts is then the total discharge of the river. This is known as a compound channel model (figure 2.2). Each of the three sections can have a different bottom roughness, depth and width. There is no interaction between the three separate channels but they do share the same water level and slope:

$$Q_{tot} = B_{mc}C_{mc}d_{mc}\sqrt{d_{mc}i} + B_{gf}C_{gf}d_{gf}\sqrt{d_{gf}i} + B_{fp}C_{fp}d_{fp}\sqrt{d_{fp}i} \qquad (2.19)$$

Q	=	Discharge	[m^3 s^{-1}]
B	=	Channel width	[m]

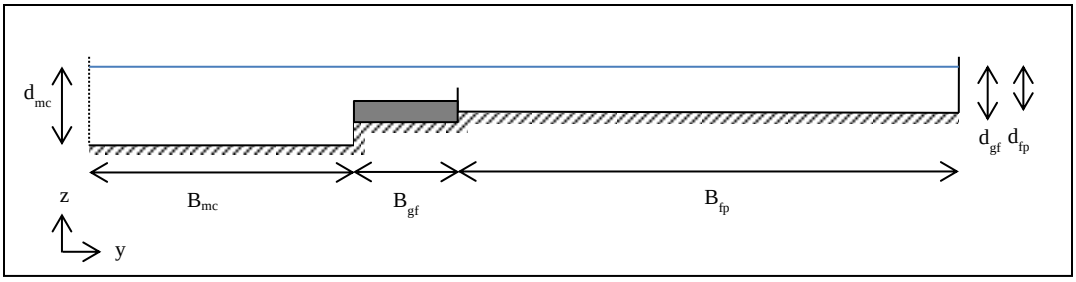

Figure 2.2: Schematization of (half of) the Waal river. The river is divided into three parts: a main channel, groyne fields and a flood plain.

A representative geometry is taken from Van der Wal (2004). These are estimates of velocity in different parts of the Waal river near Haaften (table 2.1). The total river discharge would be 10.900 m^3/s meaning the flood plains also carry water.

Table 2.3: Schematization of the Waal river at high discharge (from Van der Wal 2004).

	(Half of the) main channel	Groyne fields	Floodplain
B[m]	130	50	400
d [m]	14	8	6
Q [m^3 s^{-1}]	4550	400	500
$\bar{u}$ [m s^{-1}]	2.5	1	0.2

By assuming a $1 \cdot 10^{-4}$ slope bottom roughness can be calculated using formula 2.18. This leads to a Nikuradse roughness height $k_s = 0.033$ for the main channel and 25.33 m for the flood plains. While the former seems reasonable the latter is problematic. A roughness height four times the water depth simply does not make sense. In reality the width or even the presence of the flood plain on either side of the river is not continuous and can be heavily vegetated, which might explain such a low discharge for the stated water depth. A value of 1 m is taken as the roughness height for the flood plains instead, meaning the velocities there will be higher in the model compared to the data in Van der Wal (2004).

2.3 Groynes as drag resistance

Groynes, either emerged or submerged, influence the flow in a river. It is characterized by the ratio of the distance between groynes S to the groyne length L (figure 2.3). For a ratio of S over L smaller than two a single large gyre (C) forms in the embayment. For larger ratios a secondary gyre will form near the upstream groyne (D). For very large ratios more gyres can appear. After the separation point (A) a mixing layer forms near the groyne head. The flow stagnates again when it encounters the downstream groyne (B). This mixing layer contains large eddies that exchange momentum between the main flow and the embayment. If the secondary gyre grows sufficiently large, large eddies will be shed that also join the mixing layer (Uijttewaal et al., 2001).

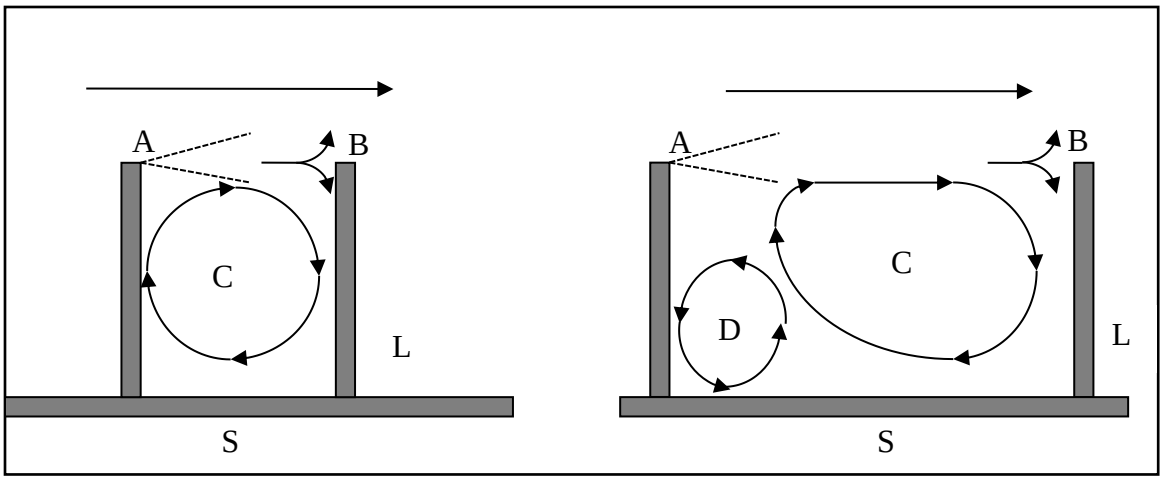

Figure 2.3: Flow near emerged groynes, left: S/L<2, right: S/L>2. Shown are the separation point after the upstream groyne (A), stagnation on the downstream groyne (B) and the primary (C) and secondary (D) gyre.

While flow in these gyres is mostly 2D, flow is strongly 3D near the interface of the main channel and the groyne tips. This does however depend on water depth. When the embayment is shallow compared to the main channel the 3D effects are stronger.

Flow in a submerged groyne field is more complex as mass and momentum can now also enter the embayment in streamwise direction over the groyne crest (figure 2.4). Lateral exchange of momentum is governed by the large eddies shed by the groyne head (C) travelling in the mixing layer (A). As a result the mixing layer has a constant width along the embayment. When water depth is low compared to crest level large gyres are still present as in the emerged case but are occasionally interrupted by flow over the groyne, but with high depths flow is constant (Uijttewaal, 2005). A large horseshoe vortex is formed in front of the groyne (B) as part of the flow is directed around the groyne while the remainder goes over it.

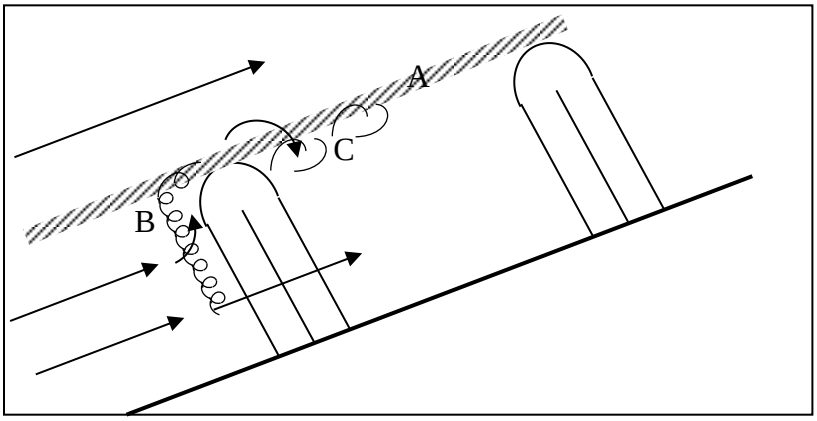

Figure 2.4: Flow near submerged groynes. Shown are the mixing layer (A), horseshoe vortex in front of the groyne (B) and eddies (C).

The issue remains of how to include their effects in the compound channel model of a river. One method is to see them as a form drag resistance (formula 2.20) and include them into the momentum equation similar to bottom resistance (formulas 2.21 and 2.22).

$$F_d = C_d A_s \rho \frac{u^2}{2} \quad (2.20)$$

F_d	=	Force due to form drag	[N]
C_d	=	Drag coefficient	[-]
A_s	=	Surface area of cross-section	[m^2]

Yossef (2005) did this and defined the cross-sectional area of the groyne as h_g/S, in effect smearing out groyne resistance over the entire length of the embayment:

$$c_{f,g} = \frac{1}{2} C_d \frac{h_g}{S} \quad (2.21)$$

h_g	=	Groyne height	[m]
S	=	Distance between successive groynes	[m]

Total resistance in the groyne fields was then defined as the sum of bottom and groyne resistance:

$$c_{f,b} = \frac{g}{C^2} \quad (2.22)$$

$$Q_{gf} = Bd \sqrt{\frac{g}{c_{f,b} + c_{f,g}}} \sqrt{di} \quad (2.23)$$

The drag coefficient C_d was then determined experimentally. Van Broekhoven (2007) used the same approach and used a numerical model to find a drag coefficient for groynes. Azinfar (2010) performed flume tests and also expressed his results as a drag coefficient but did not expand upon how to include the values into a model of a river.

2.4 Groynes as weirs

Weir formulas can also be used to represent groyne resistance. Mosselman & Struiksma (1992) defined the water level drop over a single groyne as $S \cdot i$. The reasoning being that over a long distance the water level slope in the main channel must match that of the groyne fields. Then by assuming groyne resistance is much more important than bottom resistance water level is taken to be constant between two successive groynes. The entire water level drop would then take place over the groyne (figure 2.5). Discharge over the groynes can then be calculated with a discharge formula:

$$Q_{gf} = B \cdot f(d, h_1, h_3) \quad (2.24)$$

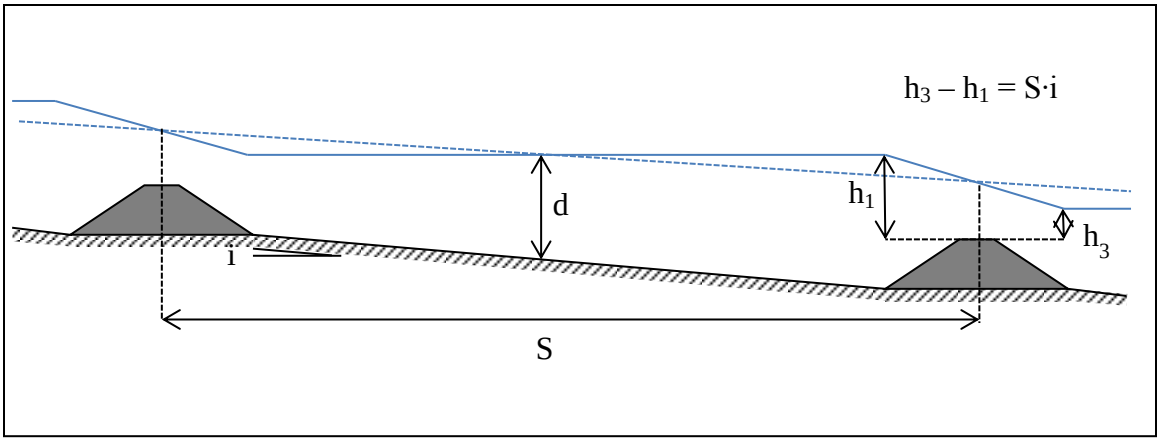

Figure 2.5: The water level drop over a groyne is assumed to be equal to the main channel slope (i) times the distance between groynes (S). The upstream (h_1) and downstream (h_3) water levels are then used to calculate the discharge according to a weir formula.

Flow over weirs is well studied in hydraulic engineering. On the upstream part of a weir (between points 1 and 2 in figure 2.6) flow accelerates. Downstream of the weir the flow decelerates which comes with an energy loss as the transfer of kinetic energy to potential energy is incomplete.

Weirs can be classified based on the Froude number (formula 2.24) over the crest and the crest length. The Froude number is the ratio of inertial forces to gravitational forces.

$$Fr = \frac{u}{\sqrt{gd}} \qquad (2.24)$$

For a Froude number above one the flow is supercritical and discharge is not a function of downstream parameters. A weir with this flow regime is called a perfect weir. Energy is dissipated in a hydraulic jump downstream. For a Froude number of one the water depth over the crest reaches a minimum. With higher downstream water levels and a resulting Froude number below one the weir becomes imperfect. Discharge over the crest is now a function of both upstream and downstream conditions.

The flow regime downstream of an imperfect weir depends on the Froude number above the crest. For values slightly below one energy is dissipated both in surface waves and in a gyre near the bottom. For lower Froude numbers the surface waves disappear and energy is dissipated in a gyre near the bottom while the main flow goes over it. Such a weir is shown in figure 2.6. Submergence is the ratio of downstream water level to upstream water level ($\frac{h_3}{h_1}$).

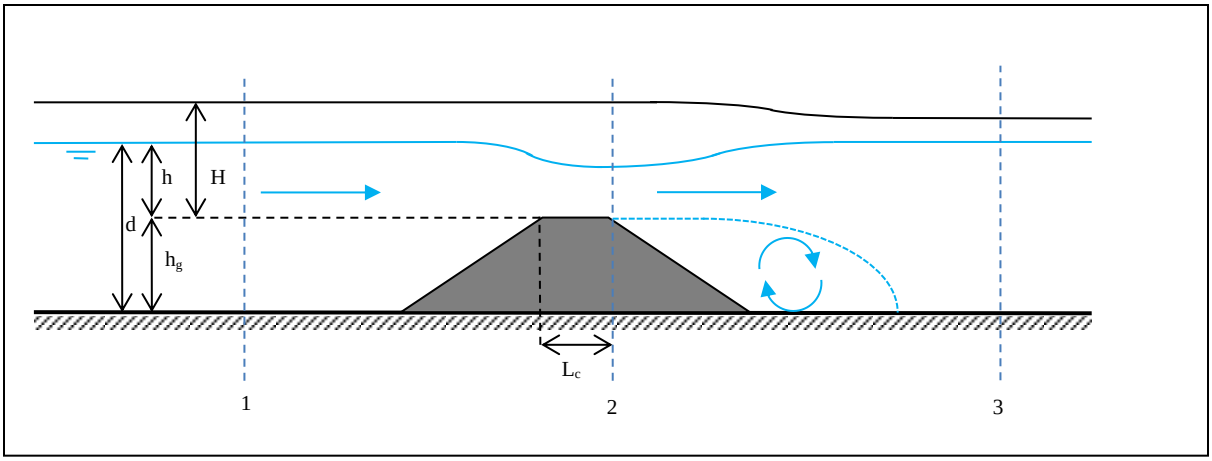

Figure 2.6: Parameters relevant for a submerged weir. Flow accelerates between areas 1 and 2. Energy is lost in a large gyre near the bottom between areas 2 and 3.

The second major aspect that determines discharge is the curvature of streamlines on the crest. For broad crests, with a length several times local water depth, flow has time to adapt to the new depth with little curvature and can be assumed to be hydrostatic. For short crests there are still significant vertical velocities and a higher discharge compared to a broad crested weir. There is a limit however as high vertical velocities can cause flow separation and vortices leading to energy loss on the crest. The ratio of the upstream energy head (formula 2.25) to crest length (L_c) is used to differentiate flow regimes.

$$H = \frac{\bar{u}^2}{2g} + h \qquad (2.25)$$

H	=	Head level above crest	[m]
h	=	Water depth above crest	[m]

Bos (1989) made the following distinction:

$H_1/L_c < 0.07$	Long crested weir
$0.07 < H_1/L_c < 0.5$	Broad crested weir
$0.5 < H_1/L_c$	Short crested weir

Flow over the weir can be considered hydrostatic if $0.07 < H/L_c < 0.5$. For values below 0.07 the weir is long enough that energy losses over the crest cannot be neglected. For values above 0.5 the vertical velocities and curvature of streamlines cannot be neglected.

One way to calculate discharge over a weir is to assume energy losses in the accelerating part of the flow at the front slope are negligible, while in the deceleration zone behind the weir energy loss is substantial but the pressure remains hydrostatic. Thus the energy equation can be used to describe flow over the upstream slope, while the momentum balance is used for the downstream slope. In this case simplified to the one dimensional continuity equation (2.26), momentum balance (2.27) and energy balance (2.28).

$$q = \bar{u}_1 d_1 = \bar{u}_2 d_2 = \bar{u}_3 d_3 \quad (2.26)$$

$$\frac{1}{2}\rho g\left(d_2 + h_g\right)^2 + \rho\alpha_2 \bar{u}_2^2 d_2 = \frac{1}{2}\rho g d_3^2 + \rho\alpha_3 \bar{u}_3^2 d_3 \quad (2.27)$$

$$H_1 = \frac{\beta_1 \bar{u}_1^2}{2g} + h_1 = \frac{\beta_2 \bar{u}_2^2}{2g} + h_2 \quad (2.28)$$

α	=	Correction coefficient	[-]
β	=	Correction coefficient	[-]

The formulas above make use of the depth average velocity. The coefficients α and β are introduced to compensate for the fact that velocity and momentum do indeed differ over the vertical axis. As long as the vertical velocity profile remains similar in streamwise direction and the riverbed remains relatively smooth α and β remain constant and close to 1. Solving this set of equations is possible but not straightforward as it has to be done iteratively. In this thesis this is done with Ridders' method.

In practice many discharge formulas are based on the just the energy equation. In case of a perfect weir flow over the crest is critical so the Froude number is one. Substituting $Fr_2 = \frac{\bar{u}_2}{\sqrt{g d_2}} = 1$ into formula 2.28 leads to:

$$q = \frac{2}{3}\sqrt{\frac{2}{3}g}H_1^{3/2} \quad (2.29)$$

To account for energy losses due to weir geometry a coefficient C_w can be introduced leading to the well-known formula 2.30. This coefficient is usually written as C_d in literature, but to avoid confusion with the drag coefficient, C_w is adopted here.

$$q = C_w \frac{2}{3}\sqrt{\frac{2}{3}g}H_1^{3/2} \quad (2.30)$$

Additional coefficients can be introduced to take into account for submergence. Fritz & Hager (1998) and Sieben (2003) both used this as a basis for their discharge formula. According to Van Rijn (1990) another option for imperfect weirs is to simply use the energy equation over the entire weir and add a coefficient m to take into account all energy losses (formula 2.31). This coefficient can vary between 0.8 for broad crested weirs to 1.35 for short crested ones:

$$q = m h_3 \sqrt{2g}\sqrt{H_1 - h_3} \quad (2.31)$$

A similar approach was used by Mosselman & Struiksma (1992) to make a schematized model of groynes in a river.

Faced with two different ways to calculate flow over groynes it is useful to compare the resistance each method gives. This is done by finding an equivalent drag coefficient that would give the same discharge as the chosen discharge formula for weirs. First the

discharge over the crest is calculated using the weir formula (formula 2.24). Then a dimensionless resistance coefficient is found that would give the same discharge in the Chézy formula (formula 2.32). Finally, under the assumption there is no bottom resistance in the groyne fields, an equivalent drag coefficient is determined (2.33)

$$c_{f,g} = \frac{gd^3 i}{q_{gf}^2} \tag{2.32}$$

$$C_d = \frac{2c_{f,g}S}{h_g} = \frac{2gd^3 iS}{q_{gf}^2 h_g} \tag{2.33}$$

2.5 Horizontal momentum exchange

The compound channel model of section 2.2 contains the implicit assumption is that there is no net exchange of discharge and momentum between the three channels. In reality a turbulent mixing layer would exist between two flows of different velocities. As a consequence momentum between the fast and slow moving channels is exchanged leading to a smoothing of the velocity gradient between them. This redistribution of momentum is not without consequence. Because the slower moving channel has a lower depth than the faster moving one, this smoothing out of the velocity profile leads to a net decrease in total discharge of the river, known as the kinematic effect. This is shown in figure 2.7. The blue areas mark the difference between a velocity profile with and without horizontal momentum exchange.

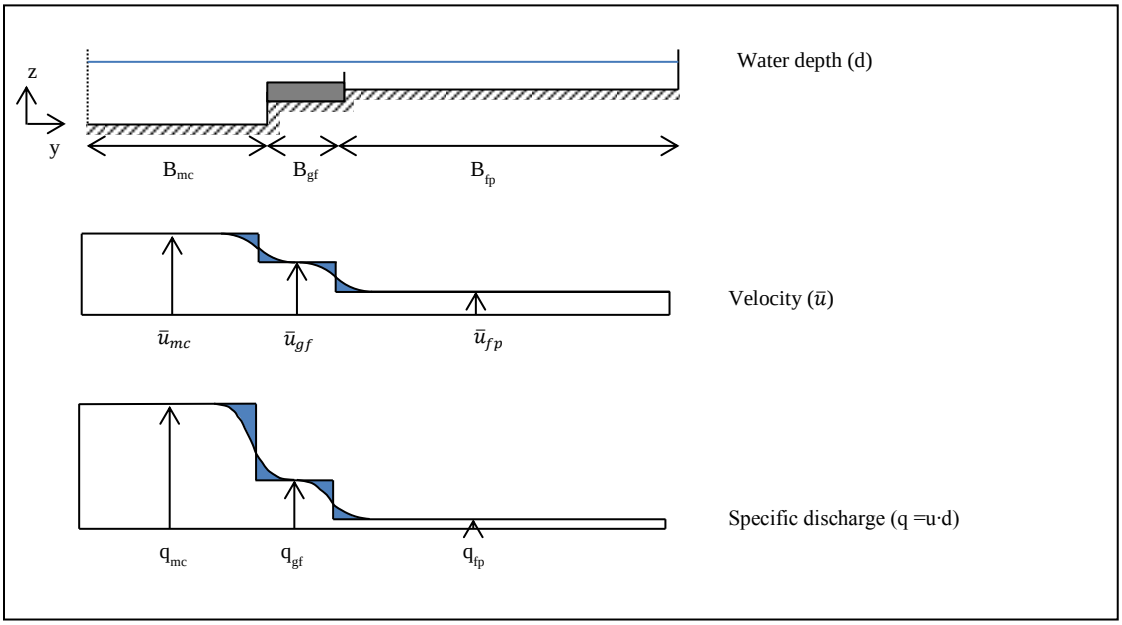

Figure 2.7: Reduction of the discharge due to horizontal momentum exchange. Blue marks the velocity and discharge exchanged between the channel sections .

It should be noted that by taking a taking into account a smoothing of the lateral velocity profile but not the bottom profile leads to an overestimation of the kinematic effect.

This effect can be replicated in a compound channel model by including the transverse momentum exchange terms of formula 2.6 into the balance of gravity and bottom resistance that made up the Chézy formula. Van Prooijen (2004) suggested the following for flow in compound channels:

$$gdi - \sqrt{\frac{g}{C^2}}\bar{u}^2 - \frac{1}{\rho}\frac{\partial \tau_{xy}}{\partial y} = 0 \qquad (2.34)$$

τ_{xy} = Transverse shear stress [N m^{-2}]

The author assumed the depth averaged turbulent shear stress would be the dominant factor and modeled it with the eddy viscosity concept as was done for the vertical Reynolds stresses in section 2.1:

$$\tau_{xy} = \rho \upsilon_t \frac{\partial \bar{u}}{\partial y} \qquad (2.35)$$

$$\upsilon_t = l_m^2 \frac{d\bar{u}}{dy} \qquad (2.36)$$

The mixing length in this case can be described by the width of the mixing layer and a constant of proportionality β (formula 2.37). According to Van Prooijen (2004) the coefficient β for a river varies between 0.088 to 0.124 in literature.

$$l_m = \beta\delta \qquad (2.37)$$

δ = Mixing layer width [m]

The width of the mixing layer between two regions of different velocity was defined by Uijttewaal & Booij (2000) as the velocity difference divided by the maximum velocity gradient:

$$\delta = \frac{\Delta\bar{u}}{\partial\bar{u}/\partial y} \qquad (2.38)$$

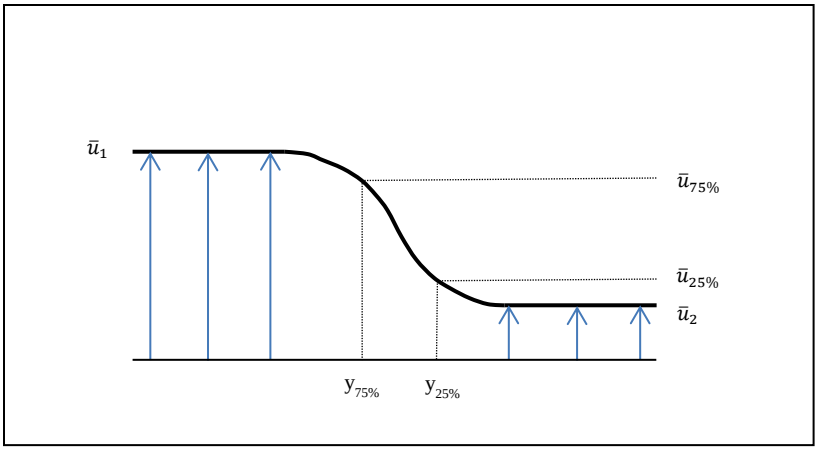

Figure 2.8 The maximum velocity gradient in the mixing layer is calculated from the points $y_{25\%}$ and $y_{75\%}$.

The maximum velocity gradient is determined from the lateral velocity profile according to figure 2.8. Between the two regions the velocity difference is given by:

$$\Delta\bar{u} = \overline{u_1} - \overline{u_2} \tag{2.39}$$

The velocity gradient is determined by two points ($y_{25\%}$ and $y_{75\%}$) in the mixing layer where the velocity is equal to:

$$\bar{u}_{25\%} = \overline{u_2} + \frac{1}{4}\Delta\bar{u} \tag{2.40}$$

$$\bar{u}_{75\%} = \overline{u_1} - \frac{1}{4}\Delta\bar{u} \tag{2.41}$$

Van Broekhoven (2007) integrated formula 2.34 over the river width to create a compound channel model which included the kinematic effect. The turbulent shear stresses were then taken as a function of the velocity difference between channels, leading to formula 2.42.

$$\tau_{xy} = -\rho\beta^2\Delta u|\Delta u| \tag{2.42}$$

$$gd_1i_1 - c_{f,1}\bar{u}_1^2 - \frac{d_2}{B_1}\beta^2(\bar{u}_1 - \bar{u}_2)|\bar{u}_1 - \bar{u}_2| = 0 \tag{2.43}$$

$$gd_2i_2 - c_{f,2}\bar{u}_2^2 - \frac{d_2}{B_2}\beta^2(\bar{u}_2 - \bar{u}_1)|\bar{u}_2 - \bar{u}_1| = 0 \tag{2.44}$$

Van Broekhoven (2007) used formulas 2.43 and 2.44 to describe flow in a two channel river. For a three channel model, with $d_{mc} > d_{gf} > d_{fp}$ the following set of equations can be used:

$$u_{mc} = C_{mc}\sqrt{d_{mc}i - \frac{d_{mc}+d_{gf}}{2B_{mc}g}\beta^2\left(u_{mc} - u_{gf}\right)\left|u_{mc} - u_{gf}\right|} \tag{2.45}$$

$$u_{gf} = \sqrt{\frac{g}{c_{f,tot}}} \sqrt{\begin{matrix} d_{gf} i - \frac{d_{mc}+d_{gf}}{2B_{gf}g} \beta^2 \left(u_{gf} - u_{mc}\right)\left|u_{gf} - u_{mc}\right| \\ - \frac{d_{gf}+d_{fp}}{2B_{gf}g} \beta^2 \left(u_{gf} - u_{fp}\right)\left|u_{gf} - u_{fp}\right| \end{matrix}} \tag{2.46}$$

$$u_{fp} = C_{fp} \sqrt{d_{fp} i - \frac{d_{gf}+d_{fp}}{2B_{fp}g} \beta^2 \left(u_{fp} - u_{gf}\right)\left|u_{fp} - u_{gf}\right|} \tag{2.47}$$

This system of equations has to be solved iteratively. In this thesis this is done by using Ridder's method.

3. Formulas for groyne resistance

There are two ways to incorporate groyne resistance in a model of a river. One approach is to consider them as drag resistance. This was done by Yossef (2005), Van Broekhoven (2007) and Azinfar (2010). The other is to consider a river as a compound channel and include a discharge formula akin to a weir for a channel representing groyne fields as done by Mosselman & Struiksma (1992) while applying Chezy's law. Only submerged groynes are considered in this thesis, with water depth being sufficiently high that flow over the crest would be sub-critical.

In this chapter these and several other weir formulas will be compared to find a value for the resistance of gronyes in the Waal river. First this value will be determined for one geometry, then this geometry will be varied to see how this influences the different formulas.

3.1 Groynefield geometry

In order to compare the resistance of each formula a 1D model of a single groyne in an infinitely long groynefield is considered as explained in chapter 2.

The geometry is taken from Van der Wal (2004). It represents a cross-section of the Waal river near Haaften during high discharge. The total discharge through the river is 10.900 $m^3 s^{-1}$. The data presented in table 3.1 only concerns the flow over and between subsequent groynes. The only exception is the main channel Froude number, which is used by the formula of Yossef (2005).

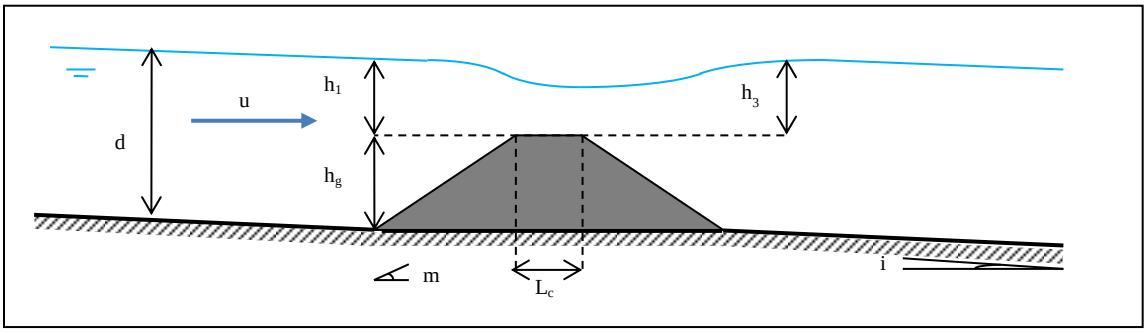

Figure 3.1: Model parameters around a groyne.

Table 3.1: Model parameters used to compare resistance.

Channel width	B_{gf}	50 m
Groyne length	L	50 m
Water depth	d	8 m
Groyne height	h_g	4 m
Bottom slope	i	$1 \cdot 10^{-4}$
Depth averaged velocity	u	1 m s^{-1}
Distance between groynes	S	200 m
Crest length	L_c	1 m
Groyne slope	m	1:3
Main channel Froude number	Fr_{mc}	0.213

3.2 Overview of formulas

A total of seven formulas were considered to represent groynes in order to find their resistance. These are listed in table 3.2 and more detailed descriptions can be found in the appendix. A summary is included below:

- Yossef (2005) used a flume with a 1:40 scale to measure velocities in between subsequent groynes and related this to the water level slope and Froude number in the adjacent main channel.

- Van Broekhoven (2007) used a computer model to simulated flow over highly submerged groynes and expressed this as a drag coefficient. Since a 2DV model was used this in essence described flow over submerged weirs expressed as a drag resistance.

- Azinfar (2010) directly measured the force on thin plates in a flume. These plates were used to represent groynes. Measurements were done at high Froude numbers (0.30 to 0.58). In addition the drag coefficient for a series of groynes was expressed relative to a uniform velocity far upstream of the groynes instead of in between subsequent groynes as Yossef (2005) did. This also makes it incompatible with the model of an infinitely long river used in this thesis. However, Azinfar (2010) did vary the width and height of the plates, as well as the distance between them.

- The formula of Mosselman & Struiksma (1992) is based on the formula for flow over submerged short crested weirs (formula 2.31) with a single coefficient m_0 to accommodate geometric and hydrodynamic influences. This coefficient can be as high as 1.3 to take into account non-hydrostatic effects above short crested weirs. This value has been used in the rest of this thesis. It was used as a first estimate

of groyne resistance in a schematized model. The upstream velocity head $\left(\frac{\bar{u}_1^2}{2g}\right)$ is neglected compared to formula 2.31 and not without consequence. While the upstream velocity head is small compared the water depth, it is large compared to the water level drop over the groyne on which the Mosselman & Struiksma (1992) formula now depends.

- The formula of Sieben (2003) was designed for summer dikes that are submerged during high discharges. These have a similar cross-section and face similar water depths as submerged groynes, making application of this formula to groynes sensible. It is based on formula 2.30 and includes two coefficients to take into account crest length (and slope) and submergence.

- Fritz & Hager (1998) developed an expansive formula to described trapezoidal weirs for a large range of situations, including high upstream and downstream water depths. This is also based on formula 2.30 and includes two coefficients to take into account crest length and submergence, though these coefficients are different than Sieben (2003).

- Finally a theoretical solution for flow over a weir is considered by calculating the energy and momentum balance over the groyne. Over the upstream slope energy is conserved (formula 2.28), while downstream of the groyne momentum is conserved (formula 2.27). Empirical constants are still needed to account for changes in the vertical flow profile, but these are not used in this thesis. Ridders' method is used to find a solution to the set of equations.

Table 3.2: Drag and weir formulas used to represent groyne resistance.

Name	Type	Formula	Validated range of water depth to groyne height ratio ($\frac{d}{h_g}$)
Yossef (2005)	Drag	$C_d = Fr_{mc}^2 76.4 \left(\frac{h_g}{d}\right)^{3.7}$	1.05 - 1.70
Van Broekhoven (2007)	Drag	$C_d = 1.79 \left(\frac{h_g}{d}\right)^2 - 0.08 \left(\frac{h_g}{d}\right) + 0.07$	2.6 - 10
Azinfar (2010)	Drag	$C_d = 1.62 \left(1 - \frac{L h_g}{B d}\right)^{-2.4} \left(\frac{h_g}{L}\right)^{-0.32} \left(\frac{d}{h_g}\right)^{-0.19}$	1.2 - 2.0
Mosselman & Struiksma (1992)	Weir	$q = m_0 (d - h_g) \sqrt{2g(h_3 - h_1)}$	-
Sieben (2003)	Weir	$q = C_w \frac{2\sqrt{2}}{3\sqrt{3}} \sqrt{g} H_1^{3/2} \sqrt{1 - \left(\frac{H_3}{H_1}\right)^p}$	1.50 - 1.75
Fritz & Hager (1998)	Weir	$q = \Psi C_w \sqrt{2g H_1^3}$	1.17 - 1.67
Energy and momentum balance	Weir	$\begin{cases} \frac{q^2}{2g d_1^2} + d_1 = \frac{q^2}{2g d_2^2} + d_2 \\ \frac{1}{2} g (d_2 + h_g)^2 + \frac{q^2}{d_2} = \frac{1}{2} g d_3^2 + \frac{q^2}{d_3} \end{cases}$	-

3.3 Resistance

The (equivalent) drag coefficient given by each formula was calculated for two different water depths and is given in table 3.3. Orange denotes that a formula is used outside the water depth to groyne height ratio it was validated for.

Table 3.3: Groyne resistance expressed as (equivalent) drag coefficient.

Formula	d = 5.4 m, d/h_g = 1.35	d = 8 m, d/h_g = 2
Yossef (2005)	1.18	0.29
Van Broekhoven (2007)	0.99	0.48
Azinfar (2010)	2.17	1.86
Mosselman & Struiksma (1998)	11.88	4.73
Sieben (2003)	12.73	4.05
Fritz and Hager (1998)	4.54	0.80
Energy and momentum Balance	11.71	2.29

The difference between the formulas is very large for both water depths, up to a factor ten at a 5.4 m. For the 8 m water depth the resistance of groynes falls somewhere around a drag coefficient of 1.5 to 4.5.

The equivalent values calculated from the weir formulas are much higher than those of the three drag formulas. This is not surprising as for weirs the entire upstream discharge is forced over the weir even at low water levels.

Drag resistance as a function of water depth over groyne height is shown in figure 3.2 for the drag resistance formulas and in figure 3.3 for the weir formulas. The dashed line represents the area where the formula is used outside of the water depth ratio (d/h_g) of the experiments it was based on. Even though the formula used by Mosselman & Struiksma (1992) has an empirical constant its validated range could not be found and thus is not dashed anywhere.

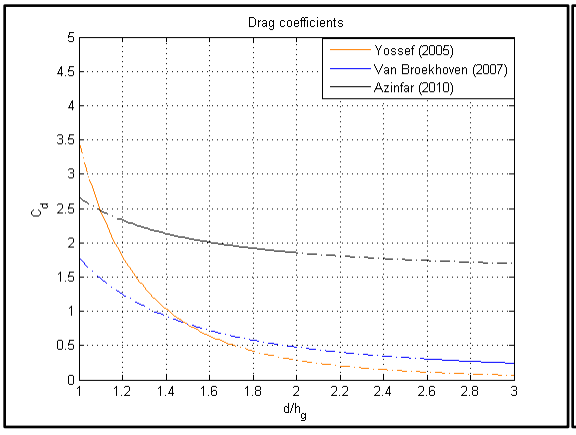

Figure 3.2: Drag coefficients of groyne formulas.

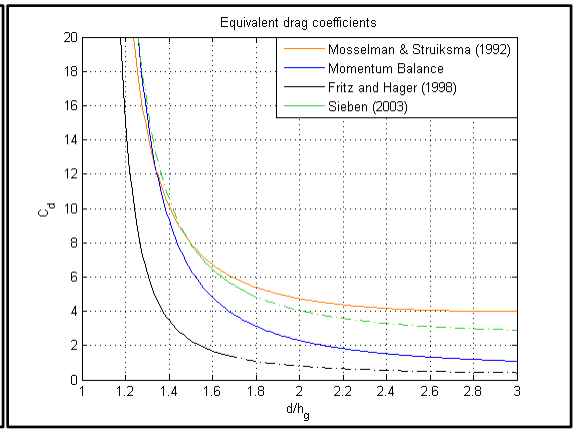

Figure 3.3: Equivalent drag coefficients of weir formulas.

The weir formulas give much higher resistance values, especially for low water depths. Again this is not unexpected as they assume all discharge flows over the crest. For high water depths Fritz and Hager (1998) and the momentum balance formulas fall into the same range as the drag formulas however.

While the formulas of Yossef (2005) and Azinfar (2010) have a nearly equal validated range they give similar values only for low water depths. The higher the water depth becomes the closer the value of the formula of Yossef (2005) comes to that of Van Broekhoven (2005), which is meant for a very high depth.

3.4 Sensitivity of formulas

In section 3.3 the resistance of different formulas was compared for a single geometry. In this section the geometry will be varied to see how the formulas scale.

Azinfar (2010) studied the drag resistance of a series of groynes and considered it to be dependent on the Reynolds number, Froude number, blockage ratio ($\frac{Lh_g}{A_s}$), aspect ratio ($\frac{h_g}{L}$), water depth ($\frac{d}{h_g}$), spacing ($\frac{S}{L}$), shape (Δ) and angle to the main flow (formula 3.1). Van Broekhoven (2007) also looked at the skin friction of groynes, but did not use this in his resistance formula.

$$C_d = f\left(Re, Fr, \frac{Lh_g}{A_s}, \frac{h_g}{L}, \frac{d}{h_g}, \frac{S}{L}, \Delta, \alpha\right) \tag{3.1}$$

Re	=	Reynolds number	[-]
Fr	=	Froude number	[-]
S	=	Distance between groynes	[m]
Δ	=	Shape factor	[-]
α	=	Angle to main flow	[°]

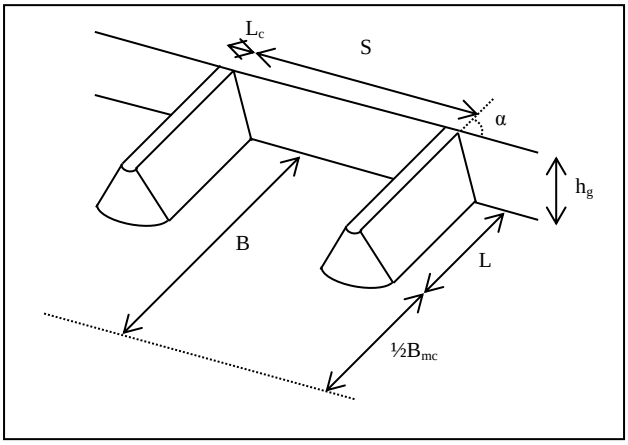

Figure 3.4: Parameters in a groyne field.

What separates submerged groynes from flow over weirs, which is more well documented, is that groynes do not extend over the full width of the flow and that they can come in series, so the first can shield the later groynes from the full impact of the flow. This introduces blockage ratio, aspect ratio and spacing as extra parameters.

Flow in rivers is considered fully turbulent, so groyne resistance is not expected to vary much with the Reynolds number. Yossef (2005) considered a 90 degree angle between main flow and groyne to be representative for the Waal river and oblique groynes are not further investigated in this thesis.

The formulas are once again included in table 3.4 along with the different parameters they depend on. Each one includes water depth and crest height. These parameters are dimensionless. In this chapter only one of the underlying properties of the geometry used in chapter 3.3 will be changed. For example: to see how the water depth to crest height ratio ($\frac{d}{h_g}$) influences groyne resistance the water depth will be changed from 4 m to 20 m, while the crest height is kept constant. These values are listed in table 3.4.

Table 3.4: Formulas and parameters they depend on.

Formula	Type	$\frac{d}{h_g}$	$\frac{h_3}{h_1}$	Fr	m	$\frac{L_c}{H}$	$\frac{L}{B}$	$\frac{S}{L}$
Yossef (2005)	Drag	■		■				
Van Broekhoven (2007)	Drag	■						
Azinfar (2010)	Drag	■					■	■
Mosselman & Struiksma (1992)	Weir	■	■					
Sieben (2003)	Weir	■	■		■	■		
Fritz & Hager (1998)	Weir	■	■			■		
Energy and momentum balance	Weir	■	■			■		

Table 3.5: Parameters that will be varied in this chapter.

Parameter	Dimensionless parameter	Varied by changing	Minimum value	Value used in chapter 3	Maximum value
Water depth to groyne height ratio	$\frac{d}{h_g}$	d [m]	4.00	8.00	20.00
Submergence	$\frac{h_3}{h_1}$	h_1 - h_3 [m]	0.00	0.02	0.04
Froude number in main channel	Fr	Fr [-]	0.050	0.213	0.300
Slope	1:m	m [m]	0	1:3	1:5
Relative crest length	$\frac{L_c}{H}$	L_c [m]	0	1	8
Groyne length	$\frac{L}{B}$	L [m]	40	50	60
Distance between groynes	$\frac{S}{L}$	S [m]	50	200	300

3.4.1 Water depth

Water depth is an important parameter in both drag formulas and weir formulas. This parameter can be made dimensionless by dividing it by groyne height. Indeed all three drag formulas explicitly do this. Weir formulas do not and may behave different for different geometries even when this ratio is kept constant.

The three drag formulas differ greatly in their dependence water depth. Figure 3.5 shows groyne resistance normalized to the value used in section 3.3. While the one of Azinfar (2010) does not seem very sensitive, the formula of Yossef (2005) does. This is because Azinfar (2010) identified blockage as most important parameter, which is only partly determined by water depth.

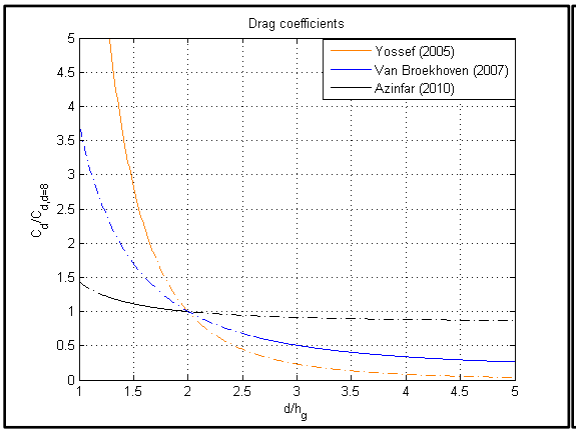

Figure 3.5: Influence of water depth on drag formulas.

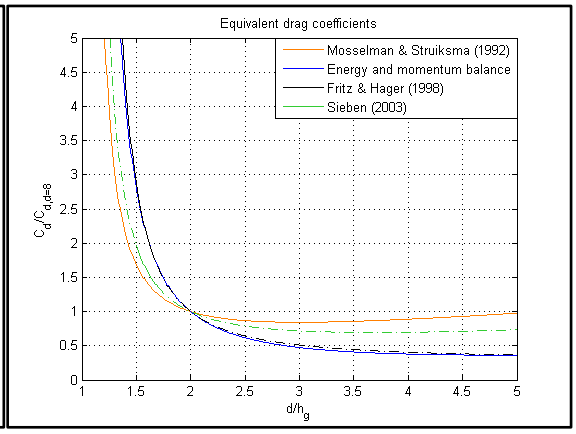

Figure 3.6: Influence of water depth on weir formulas.

The same is done for weir formulas in figure 3.6. Scaling with water depth is much closer between them, though there are differences. The formula of Mosselman & Struiksma (1992) shows increasing resistance with increasing water depth beyond a certain point. This is unwelcome because when crest height is small compared to water depth one would expect weirs to behave as a normal drag resistance with a constant drag coefficient. All other formulas seem to converge to such a constant value for increasing water depth. The reason the formula of Mosselman & Struiksma (1992) does not is because its discharge scales linearly with water depth above crest height ($d\text{-}h_g$), while discharge in Chézy's law scale with depth to the power two third ($d^{2/3}$).

The formulas of Sieben (2003) and Fritz & Hager (1998) are both based on the formula $q = C_{d,1}C_{d,2}\sqrt{2gH_1^3}$, with two coefficients for the effect of crest length and submergence. These coefficients do not change much within the range of water depth used here for the formula of Fritz & Hager (1998). Calculating the energy and momentum balance over the weir results in the nearly same scaling with water depth as the formula of Fritz and Hager (1998). This is determined by the $\sqrt{2gH_1^3}$ curve. The formula of Sieben (2003) does not show the same scaling since its coefficients vary with water depth.

The resistance of the weir formulas approaches infinity for a water depth equal to groyne height making them very sensitive at low values.

3.4.2 Submergence

All selected weir formulas depend on both upstream and downstream water level. The difference between these two is very small compared to water depth. In this model the water level drop over a groyne is given by multiplying the bottom slope and the distance between groynes (i·S), which is around 2 cm on an 8 m water depth. As such the ratio $\frac{h_3}{h_1}$ is around 0.995.

Submergence is problematic in this model for two reasons. The first has to do with how this model is set up. By incorporating groynes as a drag resistance (formula 2.33) in the Chézy formula (formula 2.35), the resulting discharge is scales with $\sqrt{iS}$. If the discharge formula that is matched with the Chézy formula does not have the same scaling the calculated drag coefficient (C_d) will instead depend on S and i. This is the case for Fritz & Hager (1998) as shown in figure 3.7. The reason for this is that its coefficient for submergence (Ψ) is not sensitive to downstream water level at high submergence. This is an unwelcome feature as neither i nor S is expected to influence the form resistance of an object unless the distance between them is sufficiently short that they influence each other's flow field. This is not the case here but will be looked at in section 3.4.7.

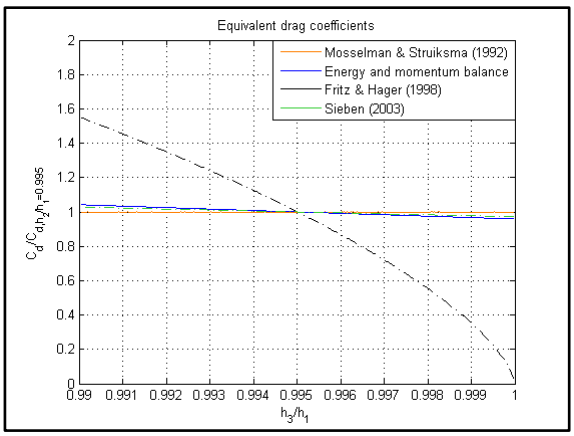

Figure 3.7: Influence of submergence on weir formulas.

The second problem is that the coefficient for submergence in the formulas of Fritz and Hager (1998) and Sieben (2003) take the shape of a power law with an exponent as calibration parameter. This is then made to fit to a data set covering a range from free overflow to fully submerged flow. Only a minority of the measurements correspond to the highly submerged groynes studied in this thesis. Figure 3.8 from Bloemberg (2001) illustrates the problem. The parameter on the x-axis corresponds to same submergence parameter h_3/h_1 used in figure 3.7. The value of the submergence coefficient is on the y-axis, which is not the same C_d used in figure 3.7. The different lines represent different values of the exponent p used to fit the data. In the groyne model used in this thesis h_3/h_1 is very close to one and the question is how well the submergence functions of Fritz & Hager (1998) and Sieben (2003) work in this area.

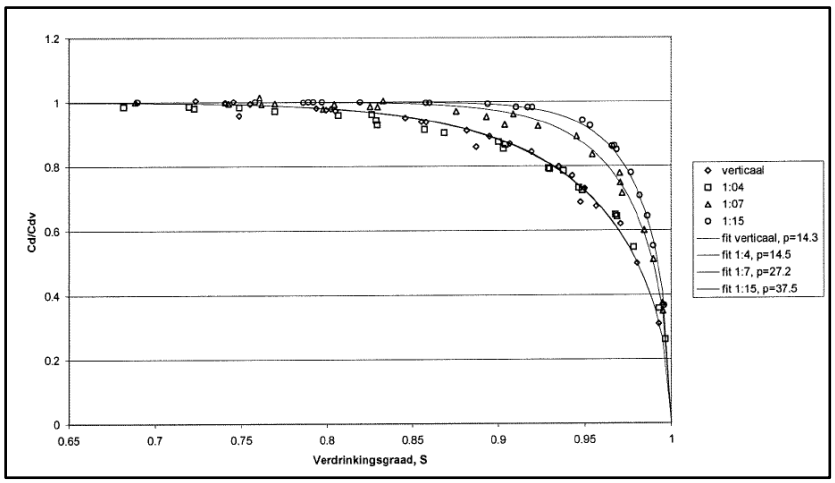

Figure 3.8: Influence of submergence on the coefficient C_w for different slopes,from Bloemberg (2001).

3.4.3 Froude number

Only the formula of Yossef (2005) varies with the main channel Froude number. It is however, a very important parameter for the formula because resistance scales with its square. While in reality a river would not vary in Froude number independently of other characteristics such as water level and slope, changing it does give insight into the behavior of the formula.

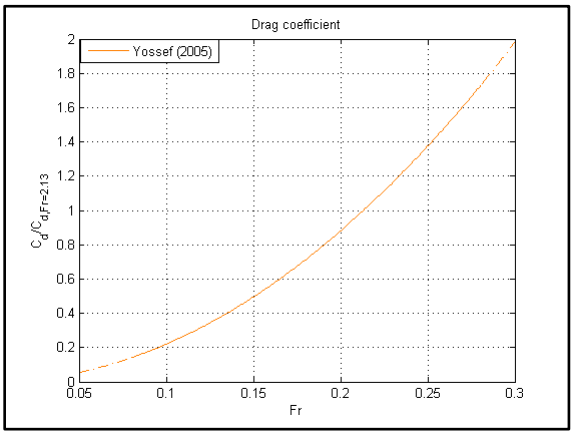

Figure 3.9: Effect of Froude number in the formula of Yossef (2005).

The results are shown in figure 3.9, where the drag coefficient is calculated relative to one at a Froude number of 0.213. This scaling is problematic. The Froude number certainly influences drag resistance of an object near the free surface, such as a weir generating undular waves. It should not matter for fully submerged objects that does not influence the surface water level. Froude number remains an important parameter regardless of water depth in this formula, which makes its application questionable when used for higher water depth to groyne height ratios than it was tested for.

Another issue is that it uses the main channel water Froude number instead the Froude number of the flow actually going over the groyne. The author does not explains how or why the main channel Froude number relates to groyne resistance.

3.4.4 Groyne slope

The formula of Sieben (2003) acknowledges the influence slopes have on discharge over a weir. This formula was proposed for the express purpose of studying the effect of streamlining embankments.

How this formula scales with different slopes is shown in figure 3.10. The equivalent drag resistance this formula gives for a one in three slope on both sides is taken as a reference point. Gentler slopes result in a lower resistance than steep slopes and this effect is more pronounced for lower water depths.

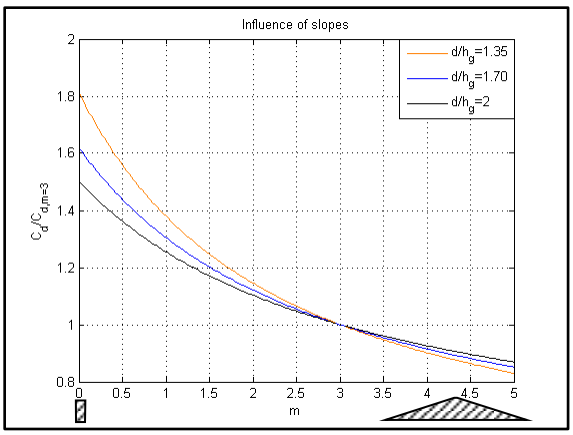

Figure 3.10: Influence of slopes in the formula of Sieben (2003).

3.4.5 Crest length

Both Sieben (2003) and Fritz and Hager (1998) included crest length as a parameter in their discharge formulas. The implementation was different. Fritz & Hager (1998) opted for a sine function while Sieben (2003) used a negative exponential formula. This is reflected in figure 3.11 which shows the equivalent drag resistance as a function of crest length normalized to the value at a crest length of 1 m. The range of the dimensionless parameter L_c/H_1 extends from zero for a sharp crested weir, to two for a broad crested weir where flow can be assumed hydrostatic.

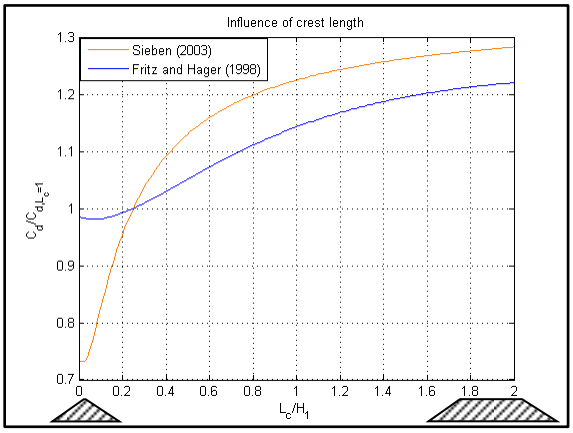

Figure 3.11: Effect of crest length in the formulas of Sieben (2003) and Fritz & Hager (1998).

The formulas disagree on the effect of crest length. The formula of Sieben (2003) attaches greater importance to it. Resistance is much lower for sharp crested weirs but increases rapidly with crest length. It is quite sensitive to crest length in the 1m range used in section 3.3. In contrast the formula of Fitz & Hager (1998) is more gradual and with less extreme values.

3.4.6 Groyne length

Only Azinfar (2010) varied groyne length in relation to channel width. This allows for a direct comparison of groyne resistance as a function of groyne length. A length of 50 m was used in section 3.3. Now a total length of 180 m is assumed for groyne length and half of the main channel combined. Groyne length is then varied from 40 to 60 m, resulting in groynes taking up 22 to 34 percent of the total length. Figure 3.12 shows the effect on the drag coefficient for different water depths. The longer groynes are relative to river width, the larger their resistance is and this effect is more pronounced with lower water depths.

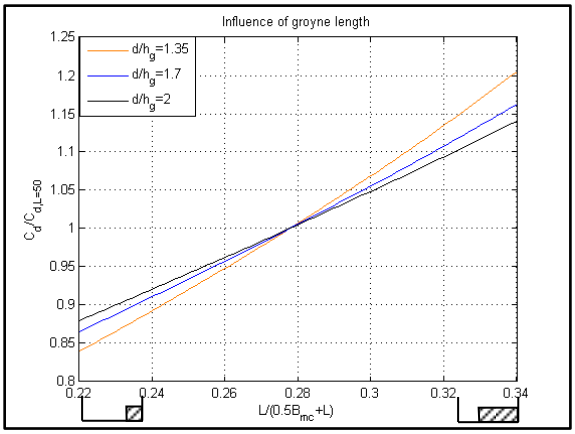

Figure 3.12: Effect of relative length based on Azinfar (2010).

3.4.7 Distance between groynes

Only Azinfar (2010) studied what effect spacing between groynes would have on resistance. He reasoned that groynes are close enough together that they influence each other's flow field, reducing each groynes resistance compared to a single groyne in the same current. The closer groynes are to each other the stronger this effect. This scaling of the formula shown in figure 3.13.

The results of the measurements of Azinfar (2010) are more complex than the figure suggests however. He compared the resistance of each groyne in a field of four to a single one for varying distances between them (figure 3.14). The resistance of the first groyne seems nearly constant, while the resistance of second decreases with increasing distance. The third groyne has, on average, the lowest resistance and this seems to increase with a relative distance above two. The fourth and final groyne shows larger resistance with increasing space.

This illustrates a problem with the drag resistance given by Azinfar (2010). It is given relative to a velocity far upstream of the groyne or groyne field. Far enough that there is no velocity difference between a main channel or groyne fields. In contrast Yossef (2005) and the model used in this thesis use a drag resistance related to the velocity upstream of a groyne inside a groyne field where there is a marked difference with the velocity of the main channel.

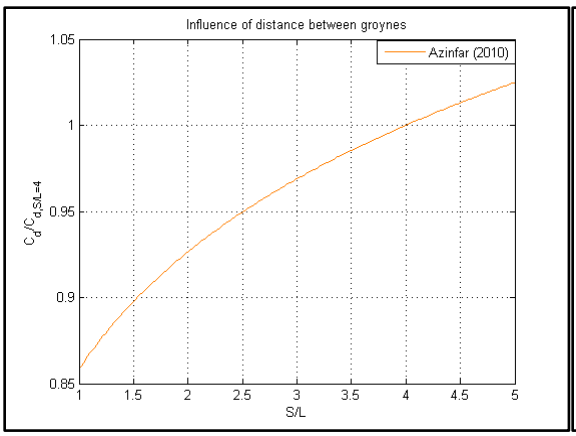

Figure 3.13: Drag coefficient as a function of relative distance between groynes.

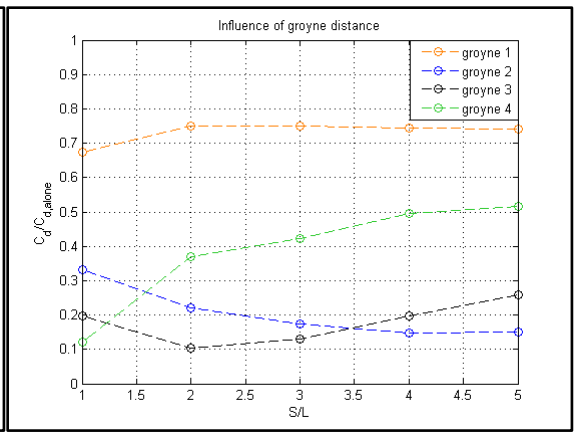

Figure 3.14: Groynes in a series compared a single groyne, data from Azinfar (2010).

It is clear that the resistance of a groyne in a field is much lower than a lone groyne, but there is much uncertainty in how much the distance between them influences this.

3.5 Conclusions

In this chapter existing groyne and weir formulas where compared to each other in a model of the river Waal. This model consisted of the Chézy equation, where in addition to bottom resistance, a drag resistance meant to represent groynes balances out the gravitational pull of the water level slope. Weir formulas could be included by assuming the water level drop over a groyne was equal to the main channel water slope times the distance between groynes.

The resistance values of the formulas differed very much. These differences increase as water depth becomes lower because weir formulas give an infinite resistance when water level is equal to crest height while the drag formulas did not. As a result no value for groyne resistance could be determined by looking at these formulas alone, though calculating the energy and momentum balance over the groyne can serve as an upper boundary. There is agreement that water depth is the most important parameter in determining resistance however.

Each of these formulas had its own shortcomings when used. The most common problem is that empirical formulas were used outside the parameter range they were validated for. Only Azinfar (2010) performed tests at the water depth to groyne height ratio considered here.

A second problem is that coupling weir formulas to a drag resistance resulted in unwanted scaling with certain parameters, which made them not directly useable. For the formula of Fritz & Hager (1998) this resulted in unwanted dependency on the distance between groynes and water level slope. For the formula of Mosselman & Struiksma (1992) this resulted in resistance increasing with water depth.

Thirdly some of the formulas themselves were suspect. The one of Yossef (2005) depends heavily on the main channel Froude number. But why this should be the case is

not explained. The formula of Mosselman & Struiksma (1992) is very similar to a well-known discharge formula for weirs, but it neglects the upstream energy height. This is not without consequences. The formula of Azinfar (2010) is not an applicable formula at all, but merely the closest fit to an expansive data set for a specific geometry. This is then related to a uniform velocity far upstream of a groyne series, making no distinction between a main channel or flow in groyne fields. In all fairness the formula is not presented as an useful engineering formula, but indeed as merely a way to describe the measured data.

The last issue has to do with crest length. Water depth above the groyne is several times the crest length in the geometry used. This would classify a weir as short. The energy and momentum balance method is valid for only for long weirs because it assumes flow is hydrostatic above the crest. The formulas of Fritz & Hager (1998) and Sieben (2003) disagree on the effect of the short crest however. The formula of Sieben (2003) is very sensitive to crest length, while that of Fritz & Hager (1998) is much less so.

Based on these factors no single formula could be found to represent groynes in the 1D schematized model. Those of Azinfar (2010), Mosselman & Struiksma (1998) and Fritz & Hager (1998) can be excluded because they do not work with the model due to unwanted parameter scaling. This is summarized below.

Table 3.6: Suitability of formulas to represent groynes in a 1D model .

Name	Type	Suitable	Why
Yossef (2005)	Drag	Maybe	
Van Broekhoven (2007)	Drag	Maybe	
Azinfar (2010)	Drag	No	Not an engineering formula. Resistance given as function of uniform upstream velocity.
Mosselman & Struiksma (1992)	Weir	No	Unwanted scaling with water depth.
Sieben (2003)	Weir	Maybe	
Fritz & Hager (1998)	Weir	No	Unwanted scaling with distance between groynes.
Energy and momentum balance	Weir	Maybe	

4 1D river model

In the previous chapter groyne resistance was looked at by comparing existing formulas for groynes and weirs. No agreement could be found however as the values the formulas gave for a geometry representing the river Waal differed. In this chapter a computer model will be used to determine groyne resistance. Due to time constraints it is not possible to model a river section with gronyes in 3D with high resolution. Therefore a single groyne will be modelled in a high resolution 2DV setup. The results will then be used to set up a schematized 1D compound channel model of the river Waal.

4.1 Computer model of flow over a single groyne

4.1.1 Model setup

The software package used is called SWASH, short for Simulating WAves till SHore. While it is, as the name suggests designed simulating waves close to the coast line it is also capable of simulating complex non-hydrostatic flows such as rivers with groynes.

The 2DV model consists of a single groyne in a 200m long channel with a bottom slope of $1 \cdot 10^{-4}$. Groyne geometry is once again taken from Van der Wal (2004) and is the same one used in chapter 3. The parameters are summarized in table 4.1. Van der Wal (2004) gives an average velocity of 2.5 m s^{-1} for the 14 m deep main channel of the river Waal. A Nikuradse bottom roughness height of 0.033 m would be needed to achieve this according to the Chézy formula (2.9). This value is also used for the model.

Table 4.1: Model parameters for 2DV simulation.

Water depth	d	5.4 - 9.3 m
Groyne height	h_g	4 m
Bottom slope	i	$1 \cdot 10^{-4}$
Distance between groynes	S	200 m
Crest length	L_c	1 m
Groyne slope	m	1:3
Bottom roughness	k_s	0.033 m

The horizontal grid size is 0.2 m so the groyne crest is covered by five meshes. Vertical discretization is achieved with ten layers of varying thickness. From top to bottom each layer is [20, 20, 15, 12, 10, 8, 6, 4, 3, 2] per cent of the water depth. Turbulence is handled by a standard k-ε model. According to Ali et al. (2012) this turbulence closure model is capable of predicting the energy head loss over weir like structures, even though it cannot accurately represent the flow profile behind it. The upstream boundary condition was a discharge, while on the downstream end a Riemann boundary was imposed.

Groyne resistance is measured by treating them as a drag resistance and setting up a control volume from 50 m before the groyne crest to 80 m behind it (figure 4.1). The change in momentum within this volume is determined by the up and downstream hydrostatic pressures, gravity, bottom resistance and drag resistance of the groyne

(formula 4.1). The average velocity 50 m upstream of the groyne is taken as reference velocity for drag resistance (formula 4.2).

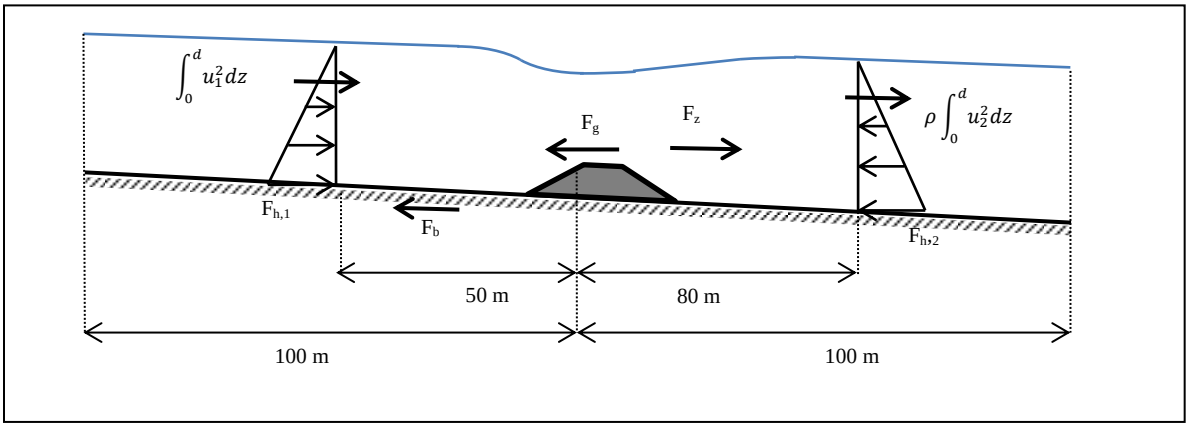

Figure 4.1: Forces acting on the control volume in the model.

$$\rho \int_0^d u_1^2 \, dz - \rho \int_0^d u_2^2 dz = F_{h,1} - F_{h,2} + F_z - F_b - F_g \quad (4.1)$$

$$F_g = \frac{1}{2} \rho C_d h_g \bar{u}_1^2 \quad (4.2)$$

ρ	=	Specific weight of water	[kg m^{-3}]
u	=	Streamwise velocity	[m s]
F_h	=	Hydrostatic pressure	[N]
F_z	=	Horizontal component of gravity	[N]
F_b	=	Bottom resistance	[N]
F_g	=	Groyne resistance	[N]

4.1.2 Results

The model was run for varying water depths ranging from 5.40 to 9.30 m. The upstream discharge was chosen so that the water level drop over the groyne would be in the order of 2 cm, though this value was up to 3 cm for some water depths. The calculated drag resistance coefficients are shown in table 4.2.

Table 4.2: Drag resistance coefficient of the groynes in the 2DV model.

Upstream water depth $d_{x,1}$ [m]	Water depth/ groyne height $d_{x,1}/h_g$ [-]	Froude number over crest Fr [-]	Average velocity 50 m upstream of groyne $\overline{u_1}$ [m s^{-1}]	Drag coefficient C_d [-]
9.30	2.33	0.30	1.19	1.01
8.65	2.16	0.30	1.06	1.25
8.00	2.00	0.34	1.00	1.41
7.35	1.84	0.34	0.83	2.01
6.70	1.68	0.33	0.65	3.20
6.05	1.51	0.39	0.54	4.64
5.40	1.35	0.39	0.34	11.31

These values are compared to four formulas in figure 4.2. These are the formulas that could potentially describe groyne resistance as determined in chapter 3.

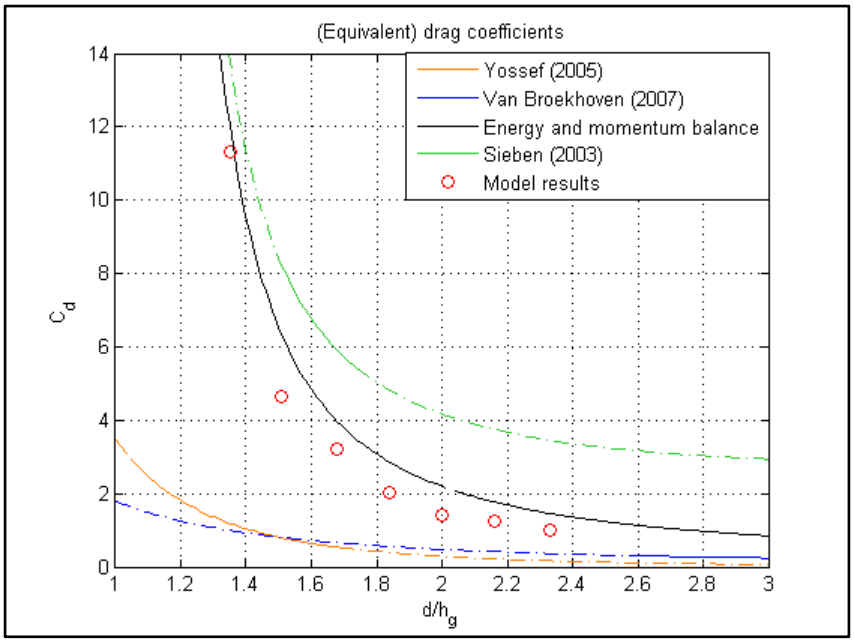

Figure 4.2: Model results compared to four formulas.

The model results come close to the values derived from calculating the energy and momentum balance over the groyne crest. The results give lower resistance values, but this is not surprising as calculating the energy and momentum balances assumes the flow above the crest is hydrostatic. In all the cases modelled here the water depth far exceeded the crest length so the groyne would be classified as a short-crested weir. Discharge over short crested weirs is higher than over short crested weirs, which would translate into a lower resistance coefficient.

However, it was also found that the curve of the formula was determined by the relationship $q \propto \sqrt{2gH_1^3}$. Thus the model results can be fit to the curve:

$$C_d = \frac{1}{A}\frac{d^3}{H_1^3} \tag{4.3}$$

A = Fitting parameter, equal to 5 [-]

The coefficient A could vary with geometry or other parameters as discussed in chapter 3, but in this case it is equal to five. For high water depths the drag coefficient converges to a constant value, as would be expected of a drag resistance. This value is 0.2 and seems low for a non-streamlined object. The model results and the fitting curve are pictured in figure 4.3.

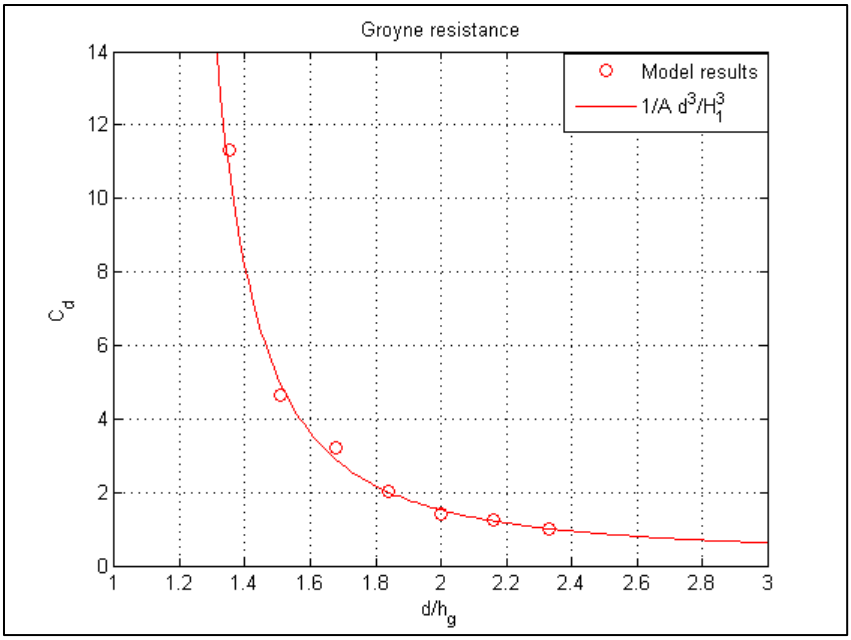

Figure 4.3: Model results and fitting curve.

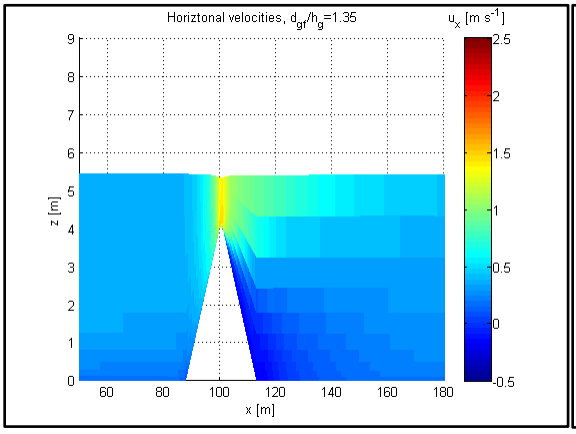

Figure 4.4: Horizontal velocities in the model at d/h_g = 1.35.

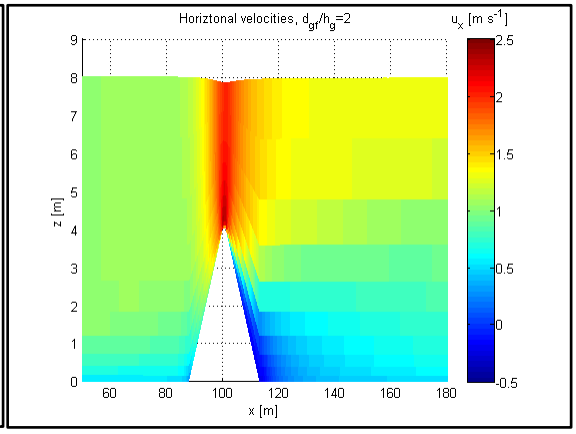

Figure 4.5: Horizontal velocities in the model at d/h_g = 2.

Horiztonal velocities for two model runs are shown in figures 4.4 and 4.5. In both cases a there is a small recirculation behind groyne.

4.2 Schematized model

Now that resistance of weirs has been determined for a geometry similar to a groyne in the Waal river this value can be used in a 1D schematized model. Knowledge of the water level is of prime importance for flood risk management. The influence of groynes can be expressed as the water level rise they cause.

4.2.1 Setup

The geometry is based on Van der Wal (2004) as explained in section 2.2. It consists of dividing the river into three parts (figure 4.6) and Chézy's law (formula 2.11) is applied to each.

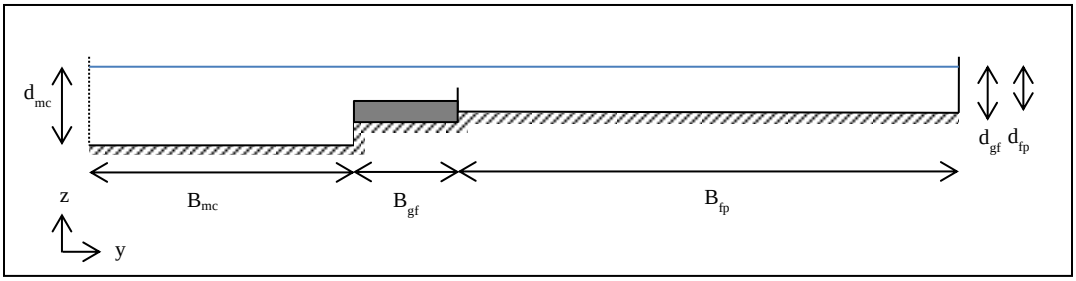

Figure 4.6: Schematization of (half of) the Waal river. The river is divided into three channels.

In the groyne fields the water level slope is assumed to be in balance with both bottom friction and groyne resistance. Drag resistance for the groyne (formula 2.21) is represented by a drag coefficient of $C_d = 1.41$ for 4 m high groynes with 200 m spacing as determined in the 2DV model. With this value bottom resistance would have to be zero to match the 1 m s^{-1} average velocity given by Van der Wal (2004). Instead a roughness height equal to that of the main channel is assumed, and as a result the velocity will be lower than in the groyne fields than stated by Van der Wal (2004).

The geometry used for the compound channel model is summarized in table 4.5. The total discharge through this hypothetical river would be 13,550 m^3 s^{-1}.

Table 4.3: Compound channel model of the river Waal.

	(Half of the) main channel	Groyne fields	Floodplain
B[m]	130	50	400
d [m]	14	8	6
Q [m^3 s^{-1}]	4550	260	1965
$\bar{u}$ [m s^{-1}]	2.5	0.65	0.82
k_s [m]	0.033	0.033	1

4.2.2 Results: bottom and groyne resistance compared

Using the previously described model the influence of bottom and groyne resistance can be compared. The discharge is kept constant at 13.550 m^3/s, which leaves the equilibrium water depth as the free variable. Groyne resistance is determined using formula 4.3 and is changed by varying groyne height from four meters to zero, at which point they are effectively removed from the model.

Bottom resistance of a river is rarely measured and it is often used as a calibration parameter in computer modeling. Sieben & Van Essen (2003) give Nikuradse roughness heights of 0.02 m in the main channel to 0.5 m near the flood plains for the Waal river.

Chézy values measured during a high discharge period were between 50 and 65 $m^{1/2}$ s^{-1}. As such 0.02 m is taken as a lower limit for roughness height. The upper limit is 0.28 m, corresponding to a main channel Chézy value of 50 $m^{1/2}$ s^{-1}. Flood plain bottom resistance remains unchanged.

Table 4.4: Water level difference due to changes in bottom and groyne resistance.

	Groyne height →	None	Low	Calibrated
Roughness height	h_g / k_s	0 m	2 m	4 m
Low	0.020 m	-0.60	-0.43	- 0.21
Calibrated	0.033 m	- 0.36	- 0.20	0.00
High ↓	0.280 m	+0.80	+0.89	+1.05

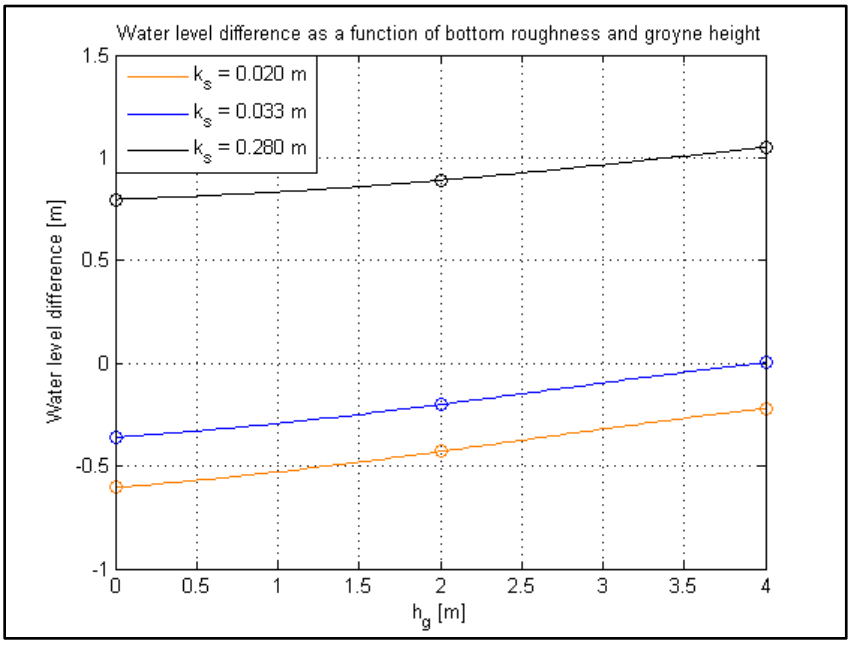

Figure 4.7: Water level difference as a function of bottom resistance and groyne height. Values of table 4.4 are marked as circles.

The change in equilibrium water level with respect to the calibrated model is listed in table 4.4. Within the chosen range changes in bottom resistance result in a larger variation of depth than groyne resistance. The low end value of bottom resistance leads to a 21 cm drop and the high end value leads to a 105 cm increase. Completely removing groynes from the model results in a 36 cm water level drop. Figure 4.7 shows this difference in water level compared to the reference situation. Taken together it shows that accurate representation of main channel bottom resistance is a more important groyne resistance.

4.3 Conclusions

A 2DV computer model was used to find the drag resistance of a heavily submerged weir. The model results came close the values obtained by calculating the energy and

momentum balance over the groyne crest. Depending on the water depth they could be up to 30% lower however. The model scaled with $\sqrt{2gH_1^3}$ in a similar way as the formula of Sieben (2003) and calculating the energy and momentum balance over the crest. For a geometry representing groynes in the river Waal resistance is given by $C_d = \frac{1}{5}\frac{d^3}{H_1^3}$.

This formula was used to represent groynes in a schematized compound channel model of the river Waal during a high discharge. With a main channel water depth of 14 m and a total discharge of 13.550 m^3, groynes are responsible for a 36 cm water level rise. However, uncertainties in bottom resistances can easily lead to larger water level variations.

5 2D river model

In the previous chapter a 1D schematized model was used to determine the influence of groynes in a river. The model divided the river in three distinct channels between which neither mass nor momentum could be exchanged. In reality this would not be the case. Due to the horizontal velocity gradient and large eddies shed by groyne heads large amounts streamwise momentum of can be exchanged between the main channel, groyne fields and flood plain. Through the kinematic effect this would alter the stage-discharge relationship of the river. Goal of this chapter is to find the magnitude of horizontal momentum exchange and determine its influence. To do that a 2DH computer model will be used.

5.1 2DH computer model

5.1.1 Model setup

The basic geometry used is once again taken from Van Der Wal (2004), the same used in previous chapters. It represents a 1400 meter stretch of the river Waal during high discharge (figure 5.1). Included are half of the main channel, seven groynes, a summer dike perpendicular to them and a flood plain.

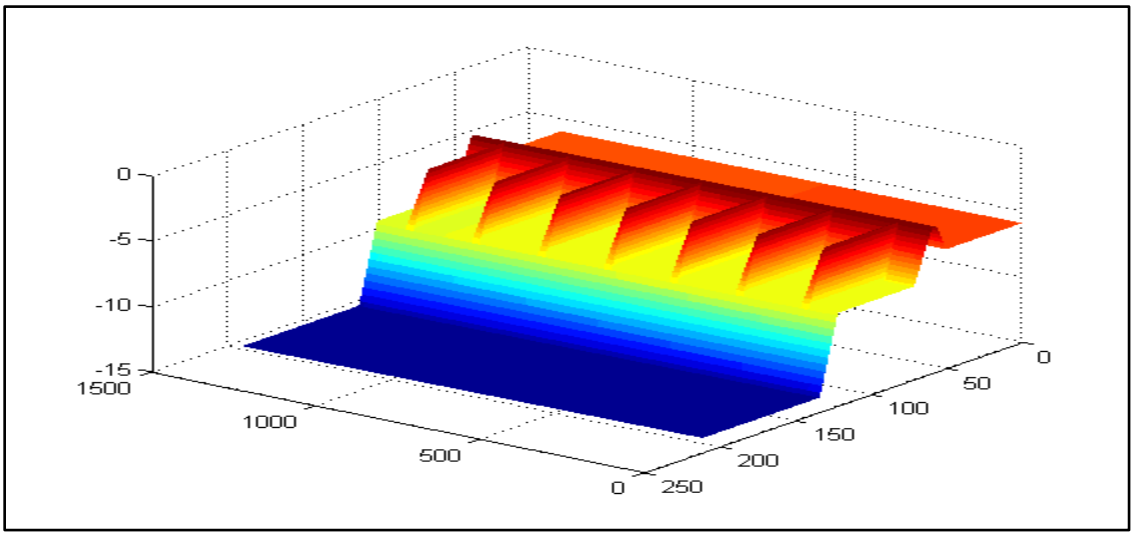

Figure 5.1: Bottom profile used in 2DH computer model. This represents half of the river's width and includes seven groynes.

Roughness height in the groyne fields was assumed identical to the main channel at 3.3 cm, just as in the previous chapter. Bottom roughness of the floodplains was kept at 1 m.

Figure 5.2 shows a cross-section of the model. The groynes themselves are 50 meters long, with a 1 meter long crest and a 1:3 slope. The slope of the summer dike was 1:3 as well, while the slope between the main channel and groyne fields was set at 1:2. Total width of the model amounts to 210 m.

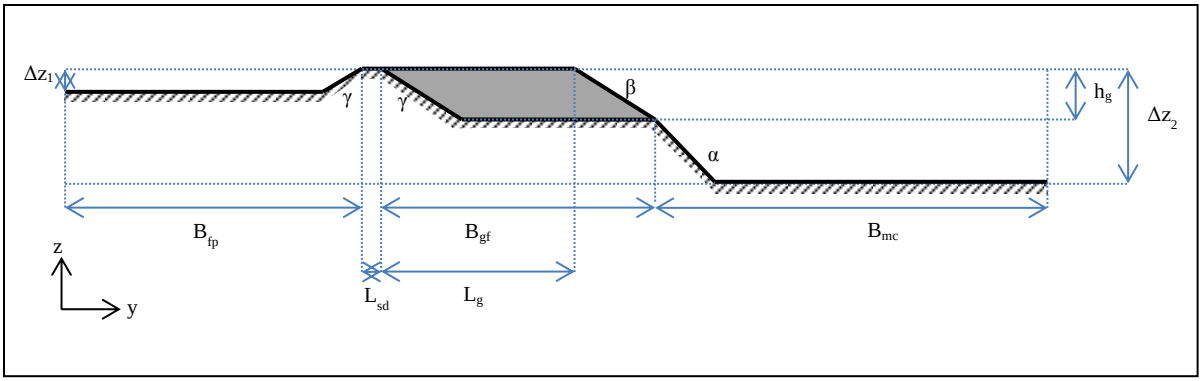

Figure 5.2: Cross-section of computer model, dashed surface is the location of the groyne.

Table 5.1: Model geometry used in 2DH computer model.

Main channel width	B_{mc}	87 m
Groyne field width	B_{gf}	62 m
Flood plain width	B_{fp}	50 m
Groye length	L_g	50 m
Summer dike crest length	L_{sd}	3 m
Height difference with flood plain	Δz_1	2 m
Groyne height	h_g	4 m
Height difference with main channel bottom	Δz_2	10 m
Slope between main channel and groyne fields	α	1:2
Groyne head slope	β	1:3
Summer dike slope	γ	1:3
Bottom level slope	i	$1 \cdot 10^{-4}$
Groyne crest length	L_c	1 m
Bottom roughness main channel	k_s	0.0326 m
Bottom roughness groyne fields	k_s	0.0326 m
Bottom roughness flood plain	k_s	1 m

The grid size is 1 m, as it could be no larger than the crest length. Ideally the crest would be covered by five meshes, but this is not feasible since the domain has to be large enough to include seven embayments, each 200 m long.

Initially multiple vertical layers were used. Turbulent exchange between these layers would be handled with a standard k-ε model. This tended to reduce the size of the gyres and a as a result the large eddies that are critical in to horizontal momentum exchange were either small or did not appear at all. Therefor the model is run in depth averaged mode. This means secondary flows cannot be studied. The influence of grid resolution is discussed in detail in section 5.1.2. A standard Smagorinsky model handles subgrid horizontal turbulent exchange. A Smagorinsky constant of 0.2 is used.

The upstream boundary condition is given by a specific discharge varied over the width of the model. The downstream is a Riemann condition to absorb large scale disturbances. Two version of this model are run. One with a 14 m main channel water depth, the other

with 11.4 m, corresponding to groyne field water depth to groyne height (d_{gf}/h_g) ratios of 2 and 1.35. These model runs are run for 1 hour. Data is gathered during the last 30 minutes.

5.1.2 Influence of grid resolution

Due to time constraints it is not possible to make a 3D model of a river with groynes with the same horizontal and vertical grid resolution used in the 2DV of section 4.1. To that end the 2DV model is revisited and grid resolution is changed to see how that influences the results.

In total the 2DV model is run in four different configurations:

- Series A is the original data set from section 4.1.2. Horizontal grid resolution is 0.2 m or five meshes per the crest length. Vertical discretization is achieved with ten layers.
- Series B has the same resolution as A, but flow is assumed hydrostatic.
- In series C horizontal resolution is increased to 1 m (one mesh per crest length) with five vertical layers. Layer thickness was [38, 27, 18, 10, 7] per cent of the water depth. Flow is assumed non-hydrostatic.
- Series D has the same horizontal resolution as C but calculations are done depth-averaged. This is the same resolution that is used in the 2DH model in this chapter .

Table 5.2: Drag resistance for various 2DV modelling options.

Series	A	B	C	D
Δx [m]	0.2	0.2	1	1
Vertical layers	10	10	5	1
Upstream water depth $d_{x,1}$ [m]	Drag coefficient C_d [-]	Drag coefficient C_d [-]	Drag coefficient C_d [-]	Drag coefficient C_d [-]
9.30	1.01	0.53	0.44	0.31
8.65	1.25	0.65	0.53	0.36
8.00	1.41	0.74	0.68	0.43
7.35	2.01	1.02	0.94	0.53
6.70	3.20	1.58	1.44	0.72
6.05	4.64	2.29	2.69	1.17
5.40	11.31	5.57	6.10	2.39

Results are also shown in figure 4.6. Neglecting non-hydrostatic pressures has a large effect on the calculated drag resistance and is not recommended. Reducing the resolution to 1 m and the amount of layers to five has a large effect on the calculated groyne resistance. This is unfortunate since this is resolution that will be used for the 3D model of chapter 6. The depth averaged resulted in very distorted resistance values.

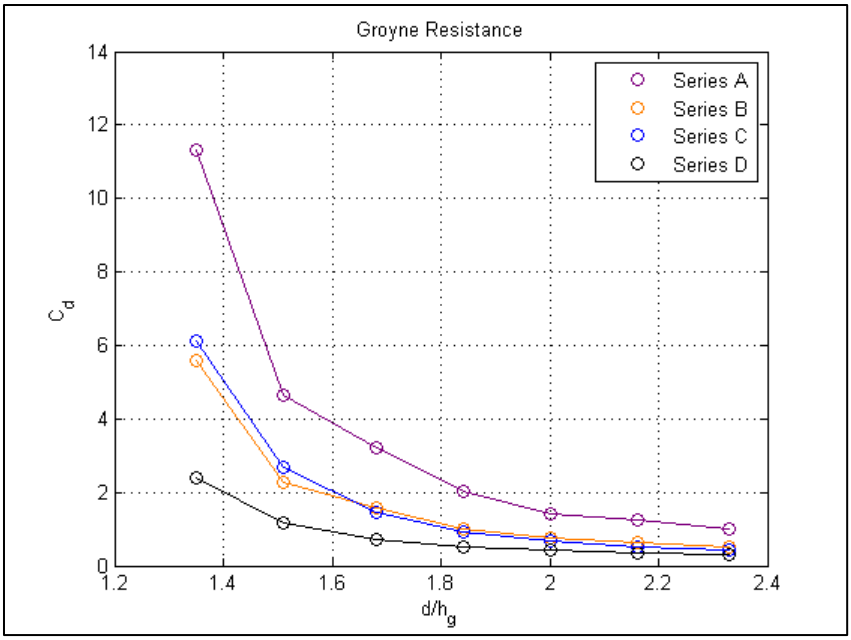

Figure 5.3: Drag resistance for 2DV various modelling options.

This is unfortunate since in order to consistently generate large eddies in the mixing layer the model needed to be run in depth averaged mode. This would result in an understatement of groyne resistance and thus change the division of discharge between the main channel, flood plains and groyne field.

To combat this the bottom roughness at the location of the groyne will be increased. The reasoning being that the total momentum lost over a groyne will be identical in a series A run and series D run, even if drag resistance alone is not. This results in a large local increase of bottom roughness, shown in table 5.3.

Table 5.3: Increase in roughness of groyne surface.

Water depth [m]	Roughness height of groyne in series A [m]	Roughness height of groyne needed in series D [m]
8.00	0.0326	2.4450
5.40	0.0326	1.4996

5.1.3 Results: average velocity

Depth and time averaged velocity is measured along a transect halfway the fourth and fifth groyne (x = 800). Results are shown in figure 5.5 for both water depths. For the high depth case the resulting velocity profile matched up reasonably well with what was assumed in the schematized model of last chapter. In the flood plain the velocity was lower however, at 0.75 m s^{-1} compared to 0.81 m s^{-1} in the schematized model.

The mixing layer between groyne fields and main channel is much wider than between the groyne fields and the flood plains. This is not unexpected as the velocity difference is

also much larger. Figure 5.4 shows the instantaneous velocity of the whole model after 15 minutes for comparison.

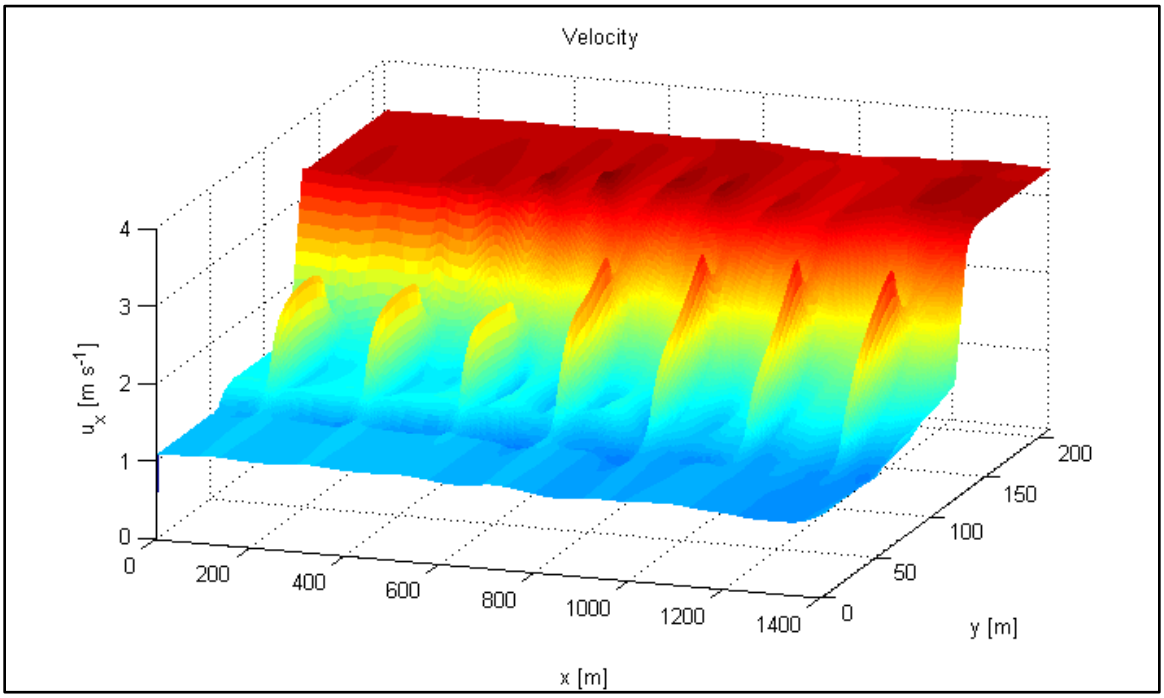

Figure 5.4: Streamwise velocity for the high water depth run of the 2DH model.

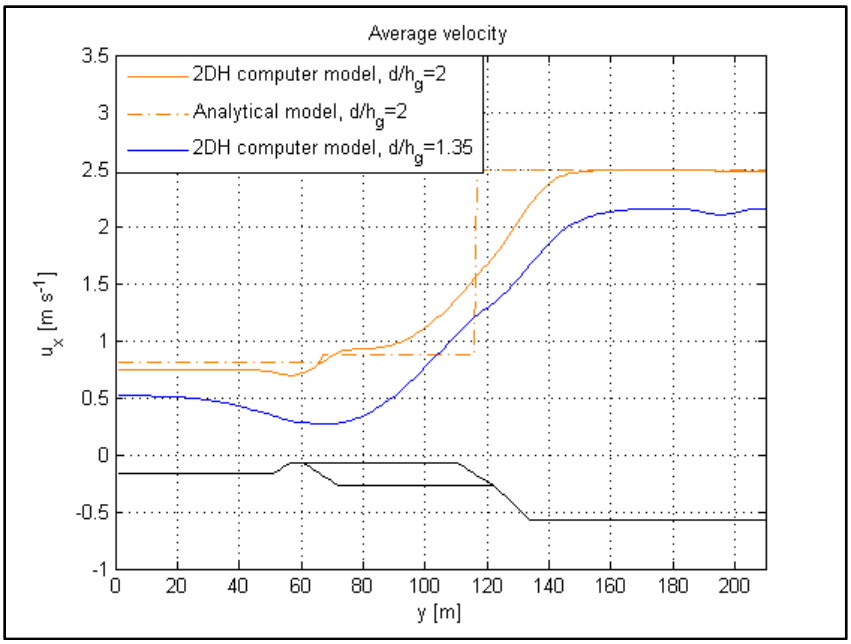

5.5: Depth and time averaged velocity profile in the 2DH model.

From these velocity profiles the mixing length and velocity gradient can be determined for both the groyne fields-flood plain interface and the groyne field-main channel interface. For the high depth case the mixing lengths are shorter and the velocity gradients are steeper than for the low depth case. These values are listed in table 5.4.

Table 5.4: Mixing layer width and velocity gradient in 2DH computer model.

Water depth	Mixing layer width δ [m]		Velocity gradient $\frac{\partial \bar{u}}{\partial y}$ [-]	
	Groyne fields-flood plain	Groyne fields-main channel	Groyne fields-flood plain	Groyne fields-main channel
$d_{gf}/h_g = 2$	13	23	$8.87 \cdot 10^{-3}$	$33.9 \cdot 10^{-3}$
$d_{gf}/h_g = 1.35$	14	32	$7.39 \cdot 10^{-3}$	$28.9 \cdot 10^{-3}$

5.1.4 Results: turbulent momentum exchange

To measure the amount of momentum exchanged in the mixing layers the area around the fifth groyne was divided into three parts (figure 5.6). Area A is the border region between the main flow and the groyne fields. It also contains the groyne head. The center area B leads up to the center of the groyne where the difference between bottom level and crest level is at its maximum of 4 m. Area C is the slope of the summer dike where the difference between bottom level and crest height is less than 4 m. This would represent the border region between the groyne fields and the flood plain. Velocities were measured in all seven transects at a rate of 4 Hz, high enough to measure all turbulence scales resolved in the momentum equation.

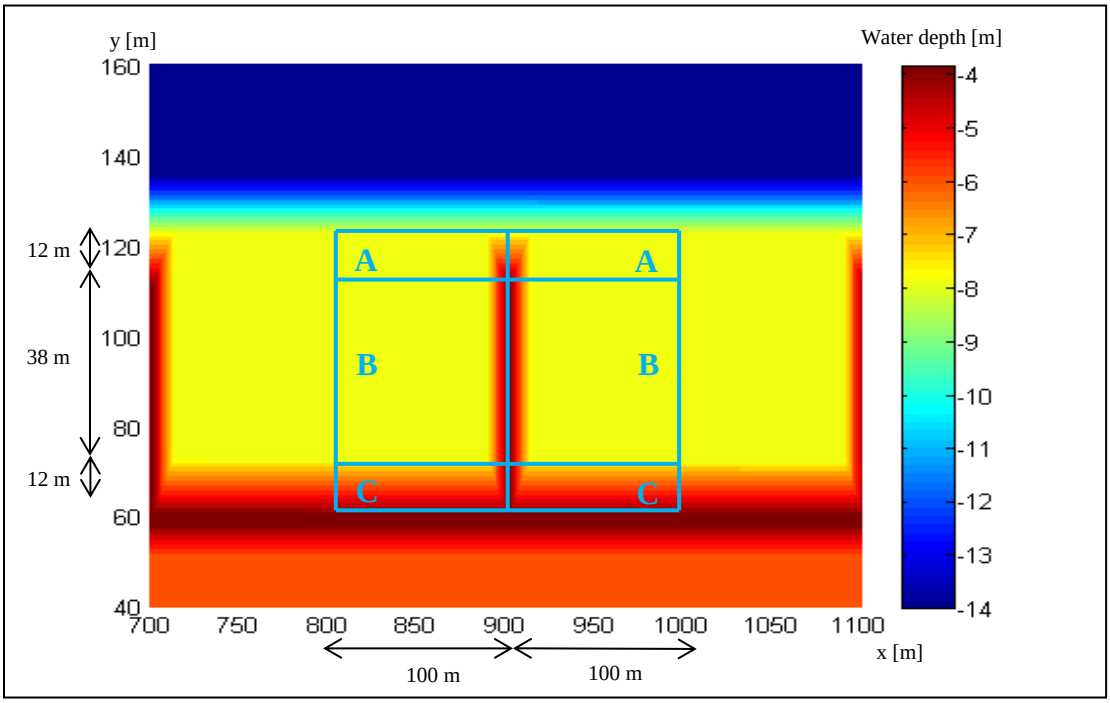

Figure 5.6: Area of interest around groyne. Data is measured along the seven transects. The area of interest is divided into three parts: (A) is the region near the main channel and includes the groyne head, (B) is the center area and (C) is the boundary area with the floodplain.

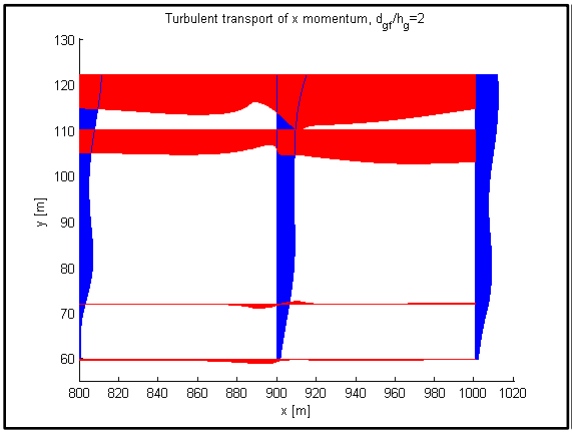

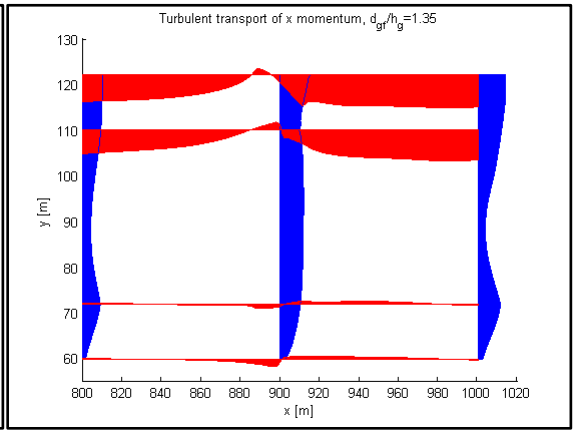

Figure 5.7: Turbulence in high depth case. *Figure 5.8: Turbulence in low depth case*

The distribution of the properties $\int_0^d \rho \widetilde{u'u'} dz$ (blue) and $\int_0^d \rho \widetilde{u'v'} dz$ (red) is shown in figures 5.7 and 5.8 for the different model runs. The $(\widetilde{...})$ symbol denotes time averaging. Sub-grid turbulence could not be included so only length scales larger than the 1 m grid size are represented here. The presence of the mixing layer is obvious in area A. Streamwise momentum is transferred from the main channel to the groyne fields almost everywhere though it is lessened just upstream of the groyne. In the low water depth case this even leads to a net flux of momentum towards the main channel. The interaction between flood plain and groyne fields is by comparison much less.

The average turbulent shear stress can be found by integration over the length of the transect and dividing it by surface area of the interface. Together with the velocity gradient and mixing layer width the value of the dimensionless constant of proportionality (formula 2.30) can be found. These values are listed in table 5.5. They are quite high, especially for the flood plain interface. Van Broekhoven (2007) found values in the range of 0.08-0.12, though he had difficulties modelling the flood plain interface as well.

Table 5.5: Magnitude of the turbulent momentum exchange in the 2DH model.

	Turbulent shear stress τ_{xy} [N m^{-2}]		Constant of proportionality β [-]	
	Groyne fields-flood plain	Groyne fields-main channel	Groyne fields-flood plain	Groyne fields-main channel
d/h_g=2	-3.78	-51.3	0.2460	0.1443
d/h_g=1.35	-1.53	-61.9	0.1954	0.1352

5.2 Schematized model

The schematized model can be expanded to take into account lateral exchange of streamwise momentum due to turbulence as explained in section 2.5. The reduction in discharge this causes is called the kinematic effect. The approach is identical to that of Van Broekhoven (2001). The streamwise velocity in each channel is given equations 2.38, 2.39 and 2.40.

These equations have to be solved iteratively and do not converge for values of β above 0.2. Since the values of β found in the model are above that for the groyne field-flood plain interface the β value found for the main channel interface will be used for both, up to a maximum of 0.144.

Table 5.7: Water level difference due to changes in turbulent momentum exchange and groyne resistance.

	Groyne height →	None	Low	Calibrated
Turbulent exchange	h_g / β	0	2	4
Calibrated ↓	0.000	- 0.36	- 0.21	0.00
	0.048	- 0.36	- 0.19	+0.06
	0.096	- 0.33	- 0.14	+0.20
Model results	0.144	- 0.28	- 0.09	+0.34

The change in equilibrium water depth due to variation in the turbulence constant and groyne resistance is shown in table 5.7. The effect of both parameters is of the same order of magnitude and they interact with each other. The higher groyne resistance is, the more turbulent exchange influence the water level and vice versa. This is not surprising as the magnitude of turbulent exchange depends on the velocity gradient. As high groyne resistance increases the velocity difference between groyne fields and main channels, so will the magnitude of momentum transferred between main channel and groyne fields. With the β value found in the 2DH computer model groynes are now responsible for a 62 cm water level difference, compared to 36 cm without including turbulent exchange. Even with the lower β value of 0.096 which is more in line with previous research, groynes result in a 53 cm difference in water level. Of course caution should be used here, changes in groyne geometry will very likely results in the mixing layer behaving differently as well which is not accounted for in this simple model. The influence of groyne resistance and momentum exchange is shown again in figure 5.11.

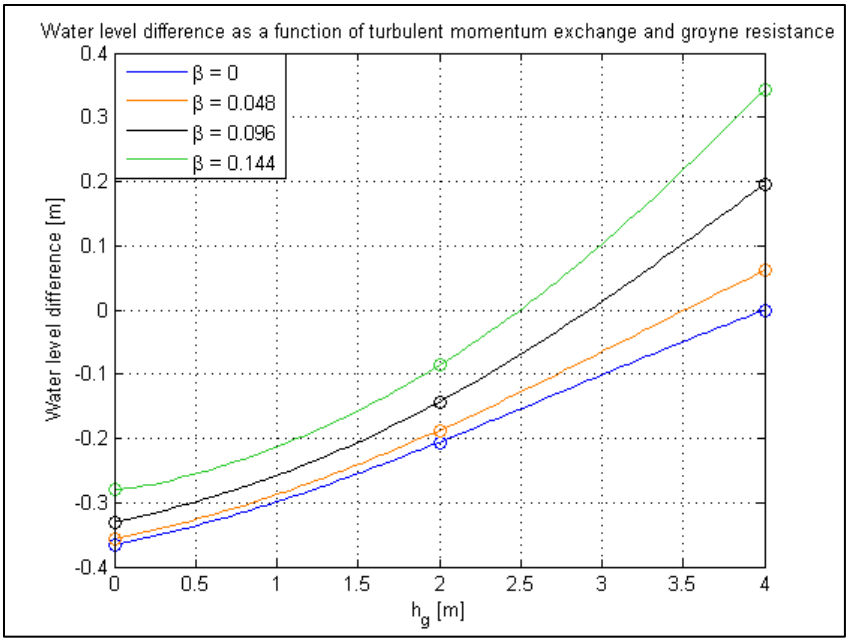

Figure 5.11: Water level difference as a function of the turbulent momentum exchange and groyne resistance. Values of table 5.7 marked by circles.

5.3 Conclusions

A 2DH computer model representing the river Waal was run with the aim of finding the horizontal velocity profile and the amount of turbulent momentum exchange through the mixing layers.

The horizontal velocity differed from what was assumed in the 1D schematized compound channel model of last chapter. This was due to the presence of a large mixing layer of 30 m. This raised velocities in the groyne fields significantly. A constant of proportionality β was found for main channel and flood plain interfaces with the groyne fields. These were 0.144 and 0.24 for 8 m water depth in the groyne fields. These are high, for comparison Van Broekhoven (2007) found values in the range of 0.08-0.12.

The effect of turbulent exchange was incorporated in the schematized model and compared to the effect of groyne resistance. Turbulent exchange of momentum in the mixing layer can reduce conveyance in a river, known as the kinematic effect. This effect is in the same order of magnitude as that of groynes. In addition their effects covary, with turbulent exchange becoming increasingly important with higher groyne resistance and vice versa. This means any river model that requires sufficient accuracy that it incorporates groyne resistance should also include the effect of turbulent momentum transfer between the groyne fields and main channel. When a high amount of turbulent exchange ($\beta = 0.144$) was included in the schematized model groynes were responsible for a 62 cm increase in water level. For a more modest value ($\beta = 0.096$) in line with previous research it is still 53 cm, compared to 36 cm when turbulent exchange is neglected.

6 3D river model

Groynes are of course three dimensional objects. In chapter 4 their resistance was determined by treating them as a weir, but flow can of course also go around them. To measure how much 3D effects around the groyne influence resistance a 3D model of a river is used.

It is the same model used in chapter 5, though with five vertical layers of varying width. From top to bottom each layer was [38, 27, 18, 10, 7] per cent of the water depth. Turbulent mixing between layers is handled by a standard k-ε model. As before two instances of the model were run with differing water depth. This configuration resulted in large eddies appearing very late in the model, or not at all for a high water depth. Therefore this 3D model will be used to only look at flow near groynes, and not at turbulent exchange in the mixing layers.

6.1 3D computer model

6.1.1 Drag resistance of groynes

Groyne resistance was measured by setting up a control volume around the fifth groyne in the model (figure 6.1). The change in streamwise momentum within this volume is determined by the up and downstream hydrostatic pressures, gravity, bottom resistance, the drag resistance of the weir and momentum fluxes through the boundaries. The approach is the same as the one used in chapter 4, but now in 3D. The average velocity in the groyne fields 100 m upstream of the groyne is taken as reference velocity for drag resistance.

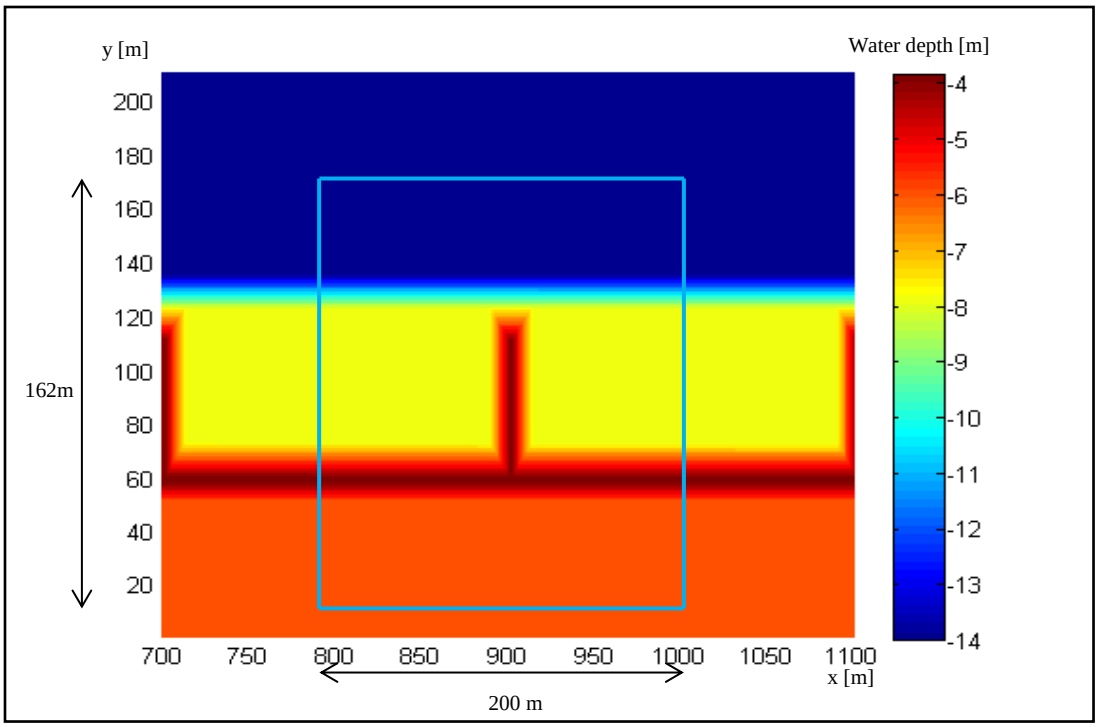

Figure 6.1: A top-down view of the fifth groyne in the high water depth computer model. The edges of the control volume are marked in blue.

This leads to drag coefficients of 0.85 and 3.82 for the high and low water depth situations (table 6.1). Compared to the drag coefficients found using the 2DV model with the same resolution the values are 25% higher and 37% lower respectively.

Table 6.1: Drag resistance coefficient of groynes.

Main channel water depth d_{mc}	Groyne field water depth/ groyne height d_{gf}/h_g	Froude number over crest Fr	Avarage velocity 100 m upstream of groyne $\bar{u}$	Drag coefficient C_d
11.4 m	1.35	0.65	0.68 m s^{-1}	3.82
14.0 m	2	0.39	1.43 m s^{-1}	0.85

Velocities upstream of the groynes were much higher than in the 2DV case which could explain some of the difference. Though the Froude number above the crest remained below 0.7 the average velocity 100 m upstream of the groyne was double that of the 2DV simulation for the low water depth. The model results of the 3D simulations are compared to the results of the 2DV simulations in figure 6.2. Series C was modelled at the same horizontal and vertical resolution as the 3D simulations.

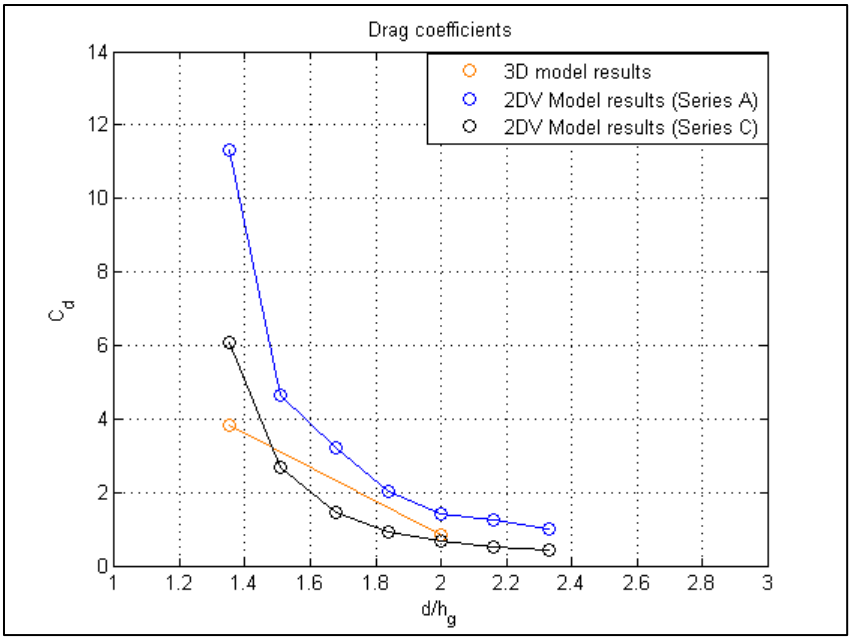

Figure 6.2: Model results of the 2DV and 3D simulations.

6.1.2 Distribution of discharge

To better understand how flow reacts to the presence of groynes the area around the fifth groyne was divided into three parts (figure 6.3) in the same fashion as chapter 5. The distribution of discharge measured along seven transects near the groyne is shown in figure 6.4 for the high depth case and figure 6.5 for the low depth case. The magnitude of flow in streamwise direction is also included in tables 6.2 and 6.3.

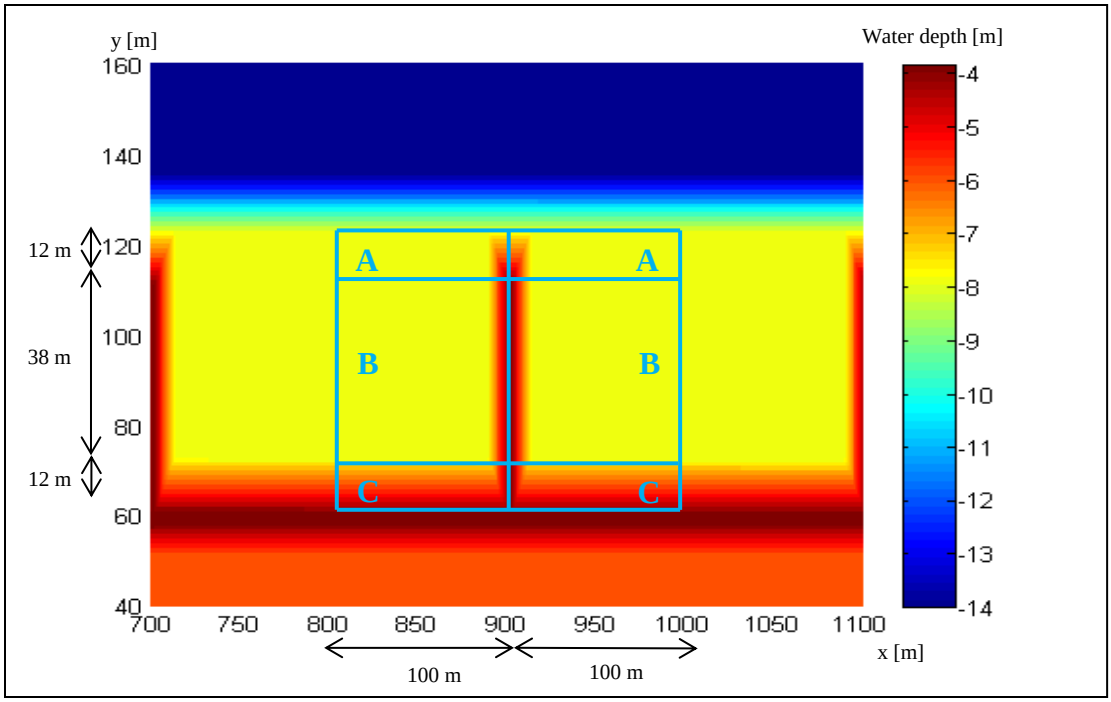

Figure 6.3: Top-down view of the area of interest around the fifth groyne. Measurements are done along the blue transects. The area of interest is divided into three parts: (A) is the region near the main channel and includes the groyne head, (B) is the center area and (C) is the boundary area with the floodplain.

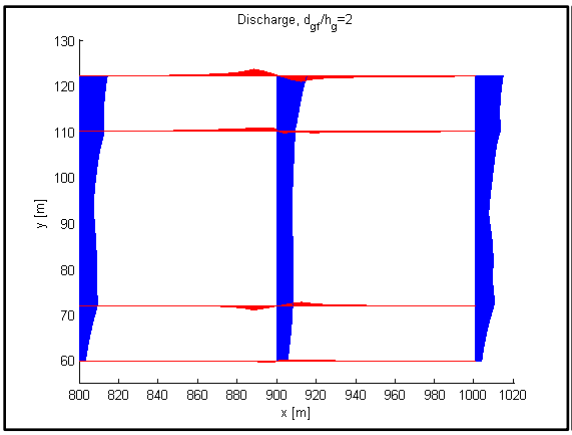

Figure 6.4: Distribution of discharge near the the fifth groyne, high depth case.

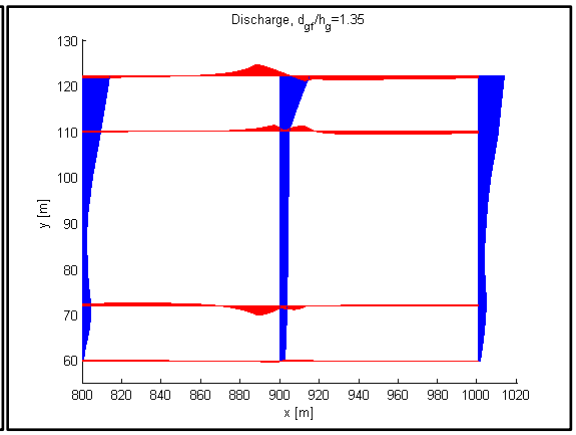

Figure 6.5: Distribution of discharge near fifth groyne, low depth case.

Table 6.2: Discharge in the groyne fields d/h_g=2.

	100 m upstream of groyne	Groyne crest	100 m downstream of groyne
Total discharge [m^3 s^{-1}]	582	545	582
% through A	27 %	27 %	27 %
% through B	61 %	58 %	61 %
% through C	12 %	15 %	12 %

Table 6.3: Discharge in the groyne fields $d/h_q=1.35$.

	100 m upstream of groyne	Groyne crest	100 m downstream of groyne
Total discharge [$m^3 s^{-1}$]	218	195	234
% through A	41 %	39 %	38 %
% through B	50 %	50 %	53 %
% through C	9 %	11 %	9 %

For the high depth case (table 6.2) 92% of the discharge 100 m upstream of fifth groyne does indeed go over groyne itself. The remaining 8% enters the adjacent main channel but just downstream of the groyne it all re-enters the groyne fields afterwards. There is little interaction with the flood plains.

In the low water depth model run (table 6.3) 84% of the upstream discharge goes over the groyne. The remaining 16% enters the adjacent main channel but downstream of the groyne much more water re-enters the groyne fields. There is little interaction with the flood plains, though a large amount of the flow does go through area C, very close to it. Compared to the high depth case a larger portion of the flow goes over the groyne head in the region near the main flow.

For the high depth case the assumption that groynes behave like weirs seems reasonable, there is little exchange of mass between the groyne fields and the main channel or flood plains, while the majority of the discharge goes over the center. In the low depth case there is more exchange with the main channel and flow over the groyne head is more important. In this case flow has a tendency to go around the groyne instead of over it, meaning groynes behave less like weirs.

6.1.3 Distribution of time averaged momentum

In addition the transport of streamwise momentum around a groyne was looked at as well. Turbulent exchange was covered in chapter 5 using a depth averaged version of the model used here.

The distribution of time averaged flux of streamwise momentum largely follows that of the division of discharge from the previous chapter. Flux in streamwise direction ($\int_0^d \rho uu\, dz$) and perpendicular direction ($\int_0^d \rho uv\, dz$) are shown in blue and red respectively in figures 6.6 and 6.7.

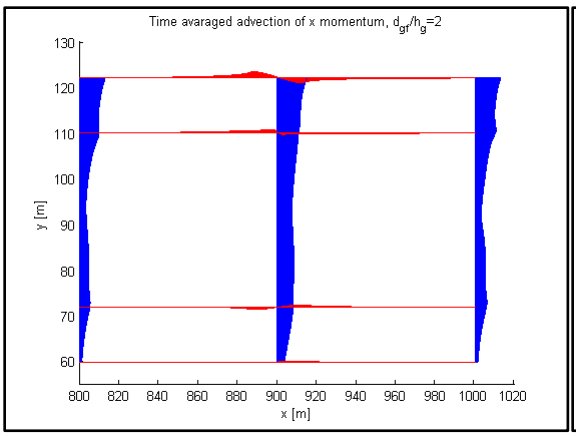

Figure 6.6: Advection of streamwise momentum, high depth case.

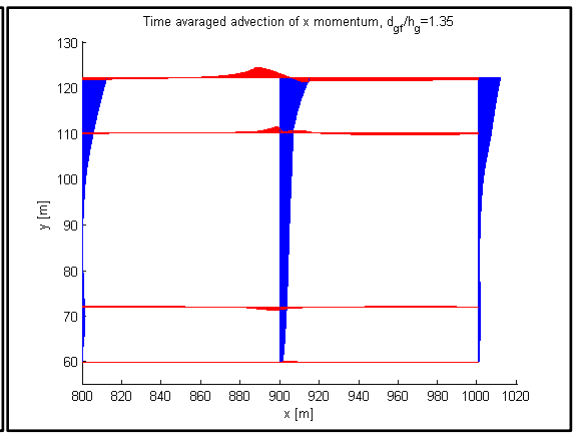

Figure 6.7: Advection of streamwise momentum, low depth case.

Table 6.4: Time averaged flux of streamwise momentum, d/h_g=2.

	100 m upstream of groyne	Groyne crest	100 m downstream of groyne
Total momentum flux [N s^{-1}]	$7.44 \cdot 10^5$	$11.23 \cdot 10^5$	$7.45 \cdot 10^5$
% through A	35 %	27 %	35 %
% through B	55 %	60 %	55 %
% through C	10 %	13 %	10 %

Table 6.4: Time averaged flux of streamwise momentum, d/h_g=1.35.

	100 m upstream of groyne	Groyne crest	100 m downstream of groyne
Total momentum flux [N s^{-1}]	$2.03 \cdot 10^5$	$3.84 \cdot 10^5$	$2.21 \cdot 10^5$
% through A	61%	36 %	55 %
% through B	33 %	55 %	40 %
% through C	6 %	7 %	5 %

Table 6.5: Lateral exchange of time averaged streamwise momentum.

Water depth	Interface	Upstream of groyne [N]	Downstream of groyne [N]	Total [N]	Average flux per m^2 [N m^{-2}]
d/h_g = 2	Groyne field-main channel	$5.98 \cdot 10^4$	$-6.04 \cdot 10^4$	-609	- 0.38
	Groyne field-flood plain	$-1.46 \cdot 10^3$	$1.59 \cdot 10^3$	-125	- 0.15
d/h_g = 1.35	Groyne field-main channel	$3.37 \cdot 10^4$	$-6.01 \cdot 10^4$	$-2.64 \cdot 10^4$	- 24.51
	Groyne field-flood plain	$-1.15 \cdot 10^3$	948	-198	- 0.71

In the high depth case this embayment seems very much in balance. The amount of streamwise momentum 100 m before the groyne is equal to that 100 m downstream, as is the distribution. 60 % of the momentum flux over the groyne goes over the crest in the center, with around a quarter going over the groyne head instead. For the low depth case this is different. Flow is more concentrated in area A near the main channel. More than one third of the total momentum flux goes over the groyne head. The groyne head plays a much more important role in the low water depth situation.

The time averaged lateral exchange of momentum was also measured (the red areas in figures 6.6 and 6.7). The results are listed in table 6.5. In the high depth case is quite obvious that a part of the streamwise momentum goes around the groyne head. There is a flux towards the main channel upstream of the groyne, which is completely cancelled out by a flux towards the groyne fields downstream. The same happens between the main channel and flood plains though the transport there is much less. Compared to the lateral turbulent flux (table 5.5) the time averaged flux is two orders of magnitude smaller and thus negligible.

The same does not hold true for the low depth case. There is a significant import of streamwise momentum from the main channel downstream of the groyne. This raises the question if the model area was long enough or if the groyne fields are simply more volatile at low water depths. In any case the time averaged flux is still less than half of the turbulent one. Interaction between groyne fields and flood plain is still minimal.

6.2 Schematized model

Now that groyne resistance has been measured in a 3D computer model the schematized model can be revisited. This is not straightforward as the resolution of the 3D model was not enough to accurately represent groynes. The 3D model results were compared to 2DV results of the same resolution however. This led to a 37% decrease and 25% increase in drag resistance for the two cases compared to the 2DV results.

Assuming the same ratio holds for a higher resolution 3D model capable of accurately representing groynes the drag coefficients would be around 7.13 for a depth of 5.4 m in the groynefields and 1.77 for 8 m water depth.

The simple relationship $C_d = \frac{1}{A}\frac{d^3}{H_1^3}$ used for the 2DV model results cannot be made to fit the two data points of the 3D model, at least not with a constant parameter A. What can be done is determining what the water level would be when consecutively groynes (with resistance based on the 2DV model), turbulent horizontal momentum exchange and 3D effects (groyne resistance measured in the 3D model) are added. The schematized cross-section of half the river is once again included in figure 6.8.

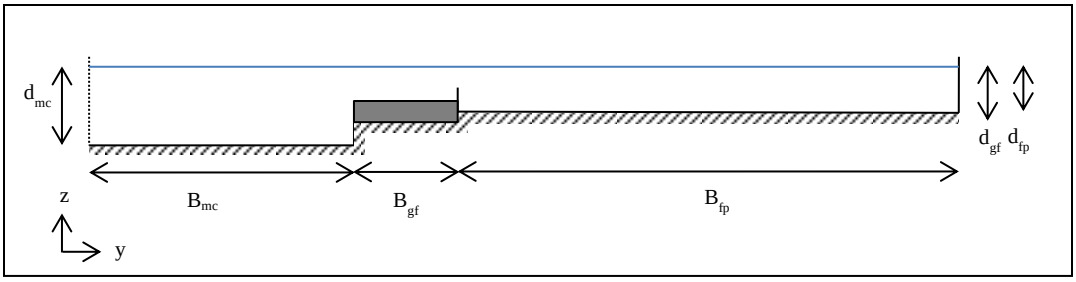

Figure 6.8: Schematization of (half of) the Waal river. The river is divided into three channels.

Results are listed in tables 6.6 and 6.7 for the same two situations used in the computer models. The high discharge corresponds to 13,550 $m^3 s^{-1}$ the lower one equals 8,095 $m^3 s^{-1}$.

Table 6.6: Water depth in the schematized model of the Waal river at high discharge.

Situation	Drag coefficient used for groynes	Main channel water depth [m]	Increase in water level [m]
Without groynes	0	13.64	-
With groynes as weir	1.41	14.00	0.36
With groynes as weir and turbulent exchange	1.41	14.34	0.34
With groynes as 3D object and turbulent exchange	1.77	14.41	0.07

Table 6.7: Water depth in the schematized model of the Waal river at low discharge.

Situation	Drag coefficient used for groynes	Main channel water depth [m]	Increase in water level [m]
Without groynes	0	11.06	-
With groynes as weir	11.31	11.40	0.34
With groynes as weir and turbulent exchange	11.31	11.94	0.54
With groynes as 3D object and turbulent exchange	7.13	11.86	-0.08

In both cases treating groynes as if they are weirs adds around 35 cm to the water level. Including turbulent exchange has around the same effect, though it is more important when the discharge is lower. Finally using the groyne resistance as found in the 3D model results in only small changes of 7 and 8 cm. In essence treating groynes as 3D objects has little added value. Using a weir formula is a reasonable approximation, especially for a higher water level, but including turbulent momentum exchange between fast flowing and slow flowing parts of the river is equally important.

6.3 Conclusions

A 3D computer model was used to simulate flow in a river with submerged groynes. Two models with different water depths were run. In the high depth case the local water depth was twice the crest height of the groynes, in the lower case this ratio was 1.35. Groyne resistance was expressed as a drag resistance with coefficients of 0.85 and 3.82 respectively. These values are 37% lower and 25% higher than those found using a 2DV model at the same resolution.

Using these values in the schematized model of the river Waal had little added value. Using resistance values found in the 2DV model gave similar water depths. Far more important is including the effect of turbulent momentum exchange between fast and slow moving parts of the river.

The time-avaraged exchange of momentum between groyne fields, main channel and floodplains was negligible in the high water depth case. Not so for the lower depth case. Exchange of streamwise momentum along groyne field-main channel interface was about half that of the turbulent transport.

In the high water depth case groynes can be seen as weirs. 92 % of the discharge in the groyne fields goes over the groyne itself and the streamwise momentum flux is more or less evenly divided over the length of the groyne.

For the low water depth case the groyne behaves somewhat different then a weir. Even though 84 % of the discharge in the groyne fields still goes over it, a significant amount is concentrated around the groyne head, meaning this part likely plays an important part in determining the total resistance of the groyne.

7 Conclusions

7.1 What is the resistance of submerged groynes and on which parameters does this depend?

Drag resistance was calculated for groynes in both a 3D and 2DV computer model. The results of the high resolution 2DV model can be described by the relationship $C_d = \frac{1}{A}\frac{d^3}{H_1^3}$, with A equal to 5.

A 3D computer model was used for two different water depths to see how much the ability of flow to go around groynes instead of over them affected resistance. Compared to values of a 2DV simulation of the same resolution the values were 37% lower at a low water depth 25% higher at a high water depth.

Based on a review of seven different formulas the most important parameter in groyne resistance was the water depth to groyne height ratio.

7.2 What is the magnitude of horizontal momentum exchange by large coherent structures?

The turbulent momentum exchange was studied with a 2DH computer model. This resulted in a mixing layer with a characteristic length in the order of 30 m between the groyne fields and the main channel and around half that for the groyne fields-floodplains interface. Values of the constant β were found of 0.14 for the main channel-groyne fields interface and up to 0.25 for the groyne fields-flood plain interface. These values are higher than in previous research. However, even if lower values are used turbulent momentum exchange is just as important for the stage-discharge relationship as groynes. The higher groyne resistance is the larger the influence of turbulent momentum exchange and vice versa. Thus any river model where sufficient accuracy is required to include groyne resistance should also include horizontal mixing.

7.3 Can groynes be seen as weirs? If so, which formulation is most applicable?

Submerged groynes can be seen as weirs. A 3D computer model was used to look at flow around submerged groynes for two different water depths. In both cases the vast majority of the discharge measured 100 m upstream went over the groyne.

The majority of the momentum flux went over the center of the groyne as well. Flux over the groyne head accounted for one quarter (high depth) to one third (low depth) of the total flux over the groyne.

Even though submerged groynes can be seen as weirs, that does not mean just any weir formula can be used to describe them. Care should be taken when using empirical formulas outside their there validated range. Seven formulas were then attempted to fit the results of a 2DV model of flow over a highly submerged weir. Calculating the energy and momentum balance over the crest gave values closest to the model results. The

model results were up to 30% lower however. This can be explained by the fact that the energy and momentum balance method described long crested weirs in which flow over the crest is assumed hydrostatic. In the parameter range studied in this thesis water depth above the groyne was always larger than crest length, which would classify them as short crested weirs.

7.4 Summary of 1D, 2D and 3D effects of groynes

A schematized model of the river Waal was set up to determine the influence of groynes on water depth. The total discharge the model had to convey was 13.550 $m^3 s^{-1}$. Groynes, when treated as weirs were responsible for a 36 cm water level rise. Including horizontal turbulent momentum exchange raised the water level by another 34 cm. Using the resistance values from the 3D model resulted in only a further 7 cm increase. In other words the added benefit of taking into account 3D effects around a groyne are small if one is interested in a stage-discharge relationship of a river. Taking into account the momentum exchange between the fast and slow moving parts is more important.

8 Recommendations

In this thesis a schematized model was created an expanded to include the 1D, 2D and 3D effects of goynes on the stage-discharge relationship of a river. The next step is to compare the results found in this thesis to flume experiments. These can be similarly divided.

- A long flume with a series of submerged weirs can be used to determine their resistance as a drag coefficient. Does the $C_d = \frac{1}{A}\frac{d^3}{H_1^3}$ relationship hold? If so, then how do submergence, crest length, Froude number and the distance between subsequent weirs influence the coefficient A?

- A wide flume can be used to find the magnitude of momentum exchange between the main channel, submerged groynes and the flood plain of a river. Key issue is then how groyne geometry and the distance between them influences this.

- The final test would be to measure the resistance of submerged groynes in a similar wide flume. This is not straightforward as it would be difficult to measure the small velocity and water level changes over a groyne unless the flume is very large. The results could be compared to the resistance of the submerged series weirs to determine experimentally if weir formulas are a valid approximation of submerged groynes.

9 References

Ali, S., Uijttewaal, W.S.J., Kimura, I. (2012). Numerical flow of rapidly varying flow over weir-like obstacles during high water discharges. Proceedings of the River Flow Conference 2012.

Anzifar, H. (2010). Flow resistance and associated backwater effect due to spur dikes in open channels. University of Saskatchewan, Saskatoon .

Bazin, H. (1888). Expériences Nouvelles sur l'Ecoulement par Déversoir. Mémoires et Documents, Annales des Ponts et Chaussées 6, pp 393-448.

Bloemberg, G. (2001). Stroomlijnen van zomerkaden. TU Delft. 77p.

Bos M.G. (1989) Discharge measurement structures. International Institute for Land Reclamation and Improvement (ILRI) Publication 20. Wageningen. 401p.

Det Norske Veritas. (2010). Environmental Conditions and Environmental Loads. Recommended Practice DNV-RP-C205.

Escande. L. (1939). Recherches nouvelles sur les barrages déversoirs noyés. La Technique Moderne 31. pp 617-620.

Fox, R.W., McDonald, A.T., Pritchard, P.J. (2004). Introduction to Fluid Mechanics. 6th Edition. John Wiley & Sons, Inc.

Fritz, H.M., Hager, W.H. (1998). Hydraulics of Embankment Weirs. Journal of Hydraulic Engineering 124, pp 963-971.

Jansen, P. P. (1979). Principles of River Engineering: The non-tidal alluvial river. Delfste Uitgevers Maatschappij. Delft.

Knight, D.W., Demetriou, J.D. (1983). Flood Plain and Main Channel Flow Interaction. Journal of Hydraulic Engineering 109. pp 1073-1092.

McCoy, A., Constantinescu, G., Weber, L. (2007). A numerical investigation of coherent structures and mass exchange processes in channel flow with two lateral submerged groynes. Water Resources Research 43. 26 p.

McCoy, A., Constantinescu, G., Weber, L.J. (2008). Numerical Investigation of Flow Hydrodynamics in a Channel with a Series of Groynes. Journal of Hydraulic Engineering 134, pp 157-172.

Mosselman, E. & Struiksma, N. (1992). Effecten van kribverlaging. WL|Delft Hydraulics, Delft.

Rehbock, T. (1929). Discussion of precise weir measurements. ASCE 93, pp 1143-1162.

Sieben, J. (1999). Energie verliezen bij zomerkaden – theoretische verkenning. Rijkswaterstaat. Werkdocument 99.151 X.

Sieben, J. (2003). Gestroomlijnde zomerkaden, de invloed van het dwarsprofiel op energieverliezen bij overlaten. Rijkswaterstaat. Werkdocument 2001.113x.

Sieben, J. & Van Essen, J.A.F. (2003). Kleinschalige morphodynamica, waarom en hoe. Rijkswaterstaat. Werkdocument 2003.060x.

Sukhodolov, A., Engelhardt, C., Kruger, A. & Bungartz. (2004). Case study: Turbulent flow and sediment distribuion in a groyne field. Journal of Hydraulic Engineering 130, 1.

Talstra, H. (2011). Large scale turbulence structures in shallow separating flows. Optima Grafische Comminicatie, Rotterdam.

Tominaga, A., Ijima, K., Nakano, Y. (2001). Flow structures around submerged spur dikes with various relative height. Proc. of 29th IAHR Congress, Beijing, China, pp 421-427.

Uijtewaal, S.S.J. & Booij, R. (2000). Efects of shallowness on the development of free-surface mixing layer. Physics of fluids. Vol 12. pp 392-402.

Uijttewaal, W.S.J, Lehmann, D. & Mazijk, A. (2001). Exchange processes between a river and its groyne fields: Model experiment. Journal of Hydraulic Engineering 127, pp 928-936.

Uijttewaal W. (2005). Effects of groyne layout on the flow in groyne fields: Laboratory experiments, Journal of Hydraulic Engineering 131, pp 782-794.

Van Broekhoven, R.W.A. (2007). Het effect van kribverlaging op de afvoercapaciteit van de Waal ten tijde van hoogwater. TU Delft, Delft.

Van der Wal, M. (2004). Innovatieve kribben met palenrijen Hoofdrapport. Rijkswaterstaat. DWW-2004-055, June 2004.

Van Prooijen, B.C. (2004). Shallow mixing layers. PrintPartners, Ipskamp.

Van Prooijen, B.C., Battjes, J.A., Uijttewaal, W.S.J. (2005). Momentum Exchange in Straight Uniform Compound Channel Flow. Journal of Hydraulic Engineering Vol. 131 No 3, March 2005.

Van Rijn, L.C. (1990). Principles of fluid flow and surface waves in rivers, estuaries, seas, and oceans. Aqua publications, Blokzijl.

Vreugdenhil, C.B. (1994) Numerical methods for shallow-water flow. Kluwer Academic Publishers, Dordrecht.

Yossef, M.F.M. (2005). Morphodynamics of rivers with groynes. Delft University Press, Delft.

Yossef, M.F.M. & De Vriend, H.J. (2011). Flow Details near River Groynes: Experimental Investigation. Journal of Hydraulic Engineering 137, pp 504.

A Drag resistance formulas

A.1 Yossef (2005)

Yossef (2005) researched the effect of lowering groyne height on river morphology. As part of this research a 1:40 scale experiment was performed with a fixed smooth bottom ($k_s = 6.27 \cdot 10^{-4}$) to measure the resistance of groynes. The model represents half a river with a series of groynes along the bank (figure A.1).

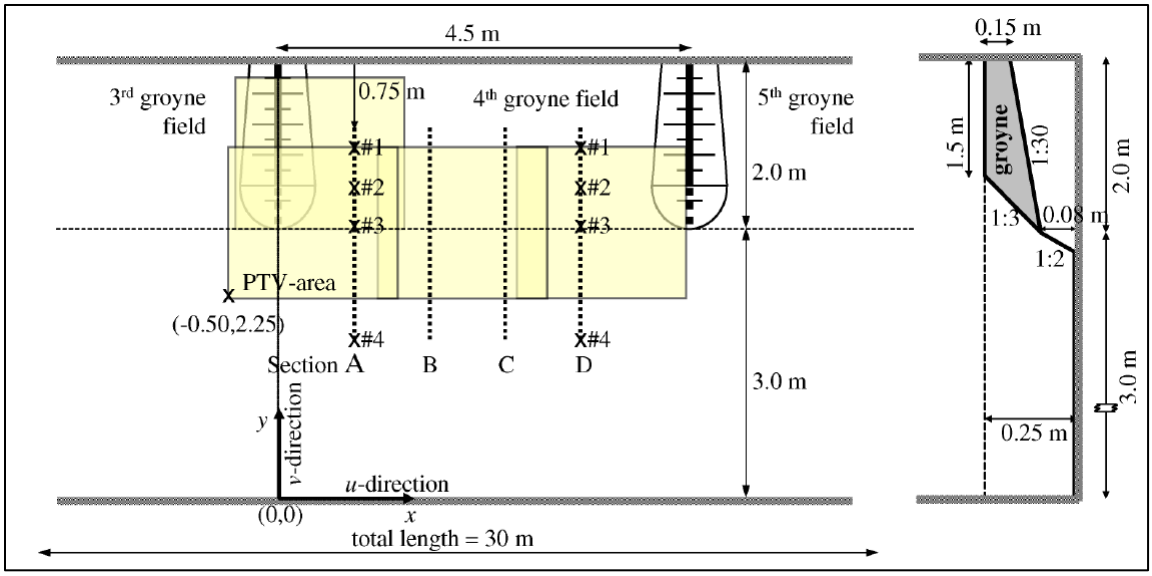

Figure A.1: Scale model setup, from Yossef & De Vriend (2005).

The velocities and water depth in the fourth groyne field as well as the water level slope in the main channel of the flume were measured. The water level drop over a groyne could not be measured as it was too small, instead it was assumed the water level slope in the groyne fields was the same as in the main channel. Drag resistance coefficient was calculated with formula A.1.

$$ghi_{mc} = \frac{g}{C^2} u_{gr}^2 + \frac{1}{2} C_d \frac{h_g}{s} u_{gr}^2 \qquad \text{(A.1)}$$

Yossef (2005) did not consider the formula of Mosselman & Struiksma (1998) useful as it required a coefficient m_0 far above 1 to fit his data. Instead he proposed to represent the resistance of weirs as a drag resistance (formula A.2). He scaled the drag coefficient of the weir with water depth and main channel Froude number. Table A.1 shows the range of parameters used in the experiments.

$$C_d = Fr_{mc}^2 76.4 \left(\frac{h_g}{d}\right)^{3.7} \qquad \text{(A.2)}$$

The flow pattern near the submerged groynes was described as an alternately accelerating pattern between flow over and around the groynes.

Table A.1: Parameter range used by Yossef (2005).

$\frac{d}{h_g}$	h_2/h_1	Fr	m	$\frac{L_c}{H}$	$\frac{L}{B}$	$\frac{S}{L}$
1.05-1.70	>0.97	0.08-0.28	1:3	?	0.4	2.25

A.2 Van Broekhoven (2007)

In order to find the effect of groyne height reduction on the capacity of the Waal river during high discharges Van Broekhoven (2007) created a 1-D schematized model and compared it to numerical 2D and 3D model results.

The 1D model was made up of three compound channels with an equal water level slope. Fluid could not be exchanged but a term was added to the momentum balance to represent the exchange of momentum in the shear layer. The resistance of groynes was modeled using a weir based formula from Mosselman & Struiksma (1992) and a drag formula from Yossef (2005). The author preferred the drag formula since the weir based formula required a large coefficient m_0 of three to give a plausible stage-discharge relation.

Van Broekhoven used a 2DH computer model to find his own function for a single groyne based on the drag method as well. He assumed the resistance to be solely a function of crest height for submerged weirs and found formula A.3.

$$C_d = 1.79\left(\frac{h_g}{d}\right)^2 - 0.08\left(\frac{h_g}{d}\right) + 0.07 \qquad \text{(A.3)}$$

He stated that bottom friction does not influence groyne resistance.

Finally he used a 3D model in FINLAB to determine the ratio of groyne resistance to total resistance and found that analytical formula to provide a good estimate.

Table A.2: Parameters range used by Van Broekhoven (2007).

$\frac{d}{h_g}$	h_2/h_1	Fr	m	$\frac{L_c}{H}$	$\frac{L}{B}$	$\frac{S}{L}$
2.6-10	>0.99	0.15-0.20	1:3	?	-	-

A.3 Azinfar (2010)

Azinfar (2010) studied the backwater effect of groynes in a 0.8 m wide flume with a smooth bottom (figure A.2). He used thin plates as groynes and placed multiples to simulate groyne fields. Velocities and water depths were measured upstream and downstream of the groynes.

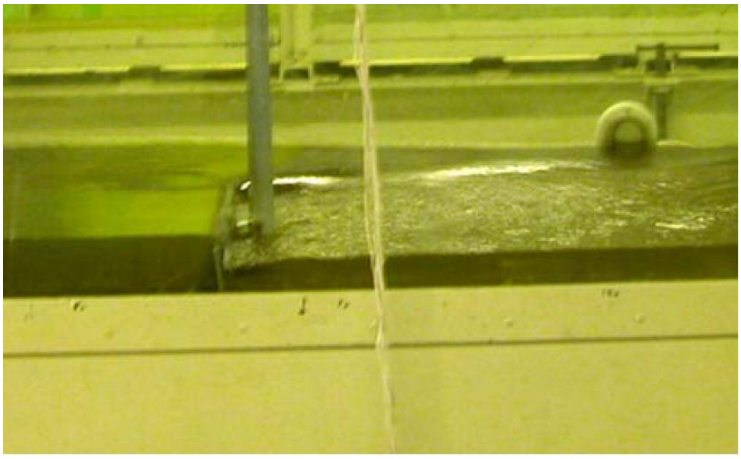

Figure A.2: Submerged plate in flume, from Azinfar 2010.

The force on groynes was both directly measured and calculated with the momentum equation using flow parameters. His data fit the following formula:

$$C_d = 1.62\left(1 - \frac{Lh_g}{Bd}\right)^{-2.4}\left(\frac{h_g}{L}\right)^{-0.32}\left(\frac{d}{h_g}\right)^{-0.19} \quad \text{(A.4)}$$

He stated that the most important parameter that determined the coefficient was the blockage ratio $A_r = \frac{Lh_g}{Bh}$. The drag coefficient also decreases with aspect ratio ($\frac{h_g}{L}$) and submergence ratio ($\frac{h_g}{d}$).

Multiple groynes were also placed in series as he believed that the first groyne would shield the subsequent groynes from the full force of the main flow if they were within a certain distance of each other. The combined drag resistance of a groyne field would therefore be likely less than the summation of individual groynes calculated with formula 3.9. The average drag coefficient of up to 15 groynes in series could be calculated by formula 3.10, but a value of m = 5 is chosen for use in this thesis.

$$C_{d,avg} = 0.78n^{-0.62}\left(\frac{d}{h_g}\right)^{0.28}\left(\frac{S}{L}\right)^{0.11} C_d \quad \text{(A.5)}$$

n = Number of groynes [-]

If the resistance of groynes would diminish with the ability of one to direct flow away from the subsequent groynes it stands to reason that this effect would scale with submergence and the distance between them. For high submergence a large part of the

flow would simply go over the groyne, while if the distance between groynes was large the main channel flow would eventually just reattach to the bank, both resulting in little shielding and high resistance.

Unfortunately the number of groynes (n) is the most important parameter in formula A.5 so it does little to describe the resistance of a groyne in an infinitely long series. Since flume length is limited fewer groynes were used for tests with high distance between them. The high value of the first groyne is thus averaged with fewer low resistance subsequent groynes. This is a possible explanation why n is the most important parameter and suggests that the influence of submergence and relative distance is understated.

A second issue is that groyne shape may influence this shielding effect. Flow could go more easily over a sloped groyne, reducing it. It should also be noted that these experiments were conducted at high Froude numbers (see table A.3), so a one to one translation to a Dutch river seems unlikely.

Table A.3: Parameter range used by Azinfar (2010).

	$\frac{d}{h_g}$	h_2/h_1	Fr	m	$\frac{L_c}{H}$	$\frac{L}{B}$	$\frac{S}{L}$
Single groyne	1.03-3.0	?	0.30-0.58	0	0	0.125-0.75	-
Groyne series	1.2-2.0	?	0.53-0.56	0	0	0.25	1-15

B Discharge formulas

B.1 Mosselman & Struiksma (1992)

Mosselman & Struiksma (1992) provided an estimate for the effect of lowering groynes on the water level during high discharges in the Waal river. They used an schematized three channel model in which they assumed resistance in the groyne fields was solely dependent on the groynes. The model did not include exchange of mass or momentum between channels. Discharge formula B.1 was used to represent groynes.

$$Q = Bm_0\left(d_{mc} - h_g\right)\sqrt{2g\Delta h} \qquad \text{(B.1)}$$

B	=	Channel Width	[m]
m_0	=	Discharge coefficient	[-]
d_{mc}	=	Water depth in main channel	[m]
Δh	=	Water level drop over groyne	[m]

The coefficient m_0 was assumed to be 1 and the effect of bottom roughness was neglected in the channel with groynes. For sharp crested groynes this coefficient can be as high as 1.3, while a bottom value for long weirs is 0.8 (Sieben, 2003). A value of 1.3 is used in this thesis. The water level drop over the groynes was given by:

$$\Delta h = iS \qquad \text{(B.2)}$$

S	=	distance between two successive groynes	[m]

B.2 Fritz and Hager (1998)

Fritz and Hager studied flow over trapezoidal weir and created an expansive discharge formula that takes into account submergence and crest length. The weir had a crest of 300 mm and crest lengths of 0, 50, 100, 200 and 300 mm were used. Submergence varied from 1.17 to 1.67 as shown in figure 3.5. The slope was a constant 1 in 2.

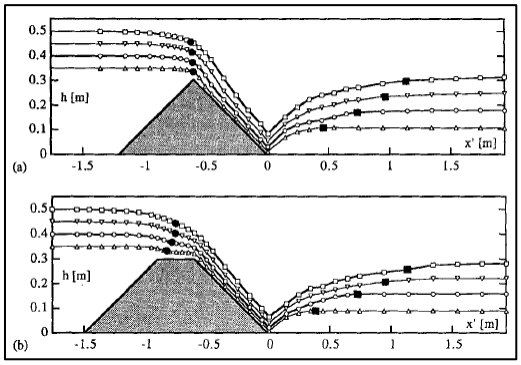

Figure B.1: Free surface profiles, from Fritz and Hager (1998).

Discharge was given by:

$$Q = \Psi C_d B \sqrt{2gH_1^3} \quad \text{(B.3)}$$

Ψ	=	Discharge reduction due to submergence	[-]
C_d	=	Discharge coefficient due to crest length	[-]

$$\Psi = (1 - Y_t)^{1/n} \quad \text{(B.4)}$$

n	=	Fitting parameter, n = 6	[-]

$$Y_t = \frac{y_t - y_l}{1 - y_l} \quad \text{(B.5)}$$

y_t	=	Submergence ratio	[-]
y_l	=	Modular limit	[-]

$$y_t = \frac{h_4}{h_1} \quad \text{(B.6)}$$

$$y_l = 0.85 - 0.5\xi \quad \text{(B.7)}$$

ξ	=	Relative crest length	[-]

$$\xi = \frac{H_1}{H_1 + L_c} \quad \text{(B.8)}$$

$$C_d = 0.43 + 0.06 sin\big(\pi(\xi - 0.55)\big) \quad \text{(B.9)}$$

$$H_1 = h_1 + \alpha \frac{u_1^2}{2g} \quad \text{(B.10)}$$

Discharge is a function of submergence through Ψ, crest length through C_d and upstream energy head H_1. For values of $H_1/h_g < 1/6$, $\alpha = 1$. For higher values $\alpha = 5/3$. The discharge coefficient depends on crest length and has a minimum of 0.33 for infinitely long crests and 0.43 for crests of zero length. The modular limit y_l is the boundary limit above which the weir can be considered drowned and also depends on crest length.

Table B.2: Parameter range used by Fritz & Hager (1998).

$\frac{d}{h_g}$	h_2/h_1	Fr	m	$\frac{L_c}{H}$	$\frac{L}{B}$	$\frac{S}{L}$
1.17-1.67	0 – 0.98	≈0.2	1:2	0 - ≈10	-	-

B.3 Momentum Balance

The discharge can also be found by solving the momentum equation over the upstream slope of the groyne (formula 2.31) and the energy equation over the downstream slope (formula 2.32) as long as it can be assumed that the water level over the crest does not change. In other words $h_2 = h_3$. In this fashion the discharge of a fully drowned, or imperfect, weir can be calculated. For a full description of the procedure see Sieben (1999). All coefficients α and β were assumed to be 1.

B.4 Sieben (2003)

To determine the effect of the shape of a weir on its discharge Sieben (2003) conducted an expansive literature review and together with laboratory tests done by Bloemberg (2001) proposed the following formula:

$$Q = C_d B \frac{2\sqrt{2}}{3\sqrt{3}} \sqrt{g} H_1^{3/2} \sqrt{1 - \left(\frac{H_4}{H_1}\right)^p} \tag{B.11}$$

$$C_d = 0.85 e^{-0.15 H_1 / L_c} (1 - 0.25 e^{-0.5 m_u}) + 0.85 \left(1 - e^{-0.15 H_1 / L_c}\right) (0.8 + 0.65 e^{-0.1 m_d}) \tag{B.12}$$

$$p = 11 + 1.6 m_d \tag{B.13}$$

m_u	=	Upstream slope	[-]
m_d	=	Downstream slope	[-]

This was used to study the influence of sloping and crest length. In the experiments only the downstream slope was varied.

Table B.3: Parameter range used by Bloemberg (2001).

$\frac{d}{h_g}$	h_2/h_1	Fr	m	$\frac{L_c}{H}$	$\frac{L}{B}$	$\frac{S}{L}$
1.50-1.75	0 - 0.99	0.03-0.18	upstream: 1:4 downstream: 0-1:15	?	-	-